SIAM J. SCI. COMPUT.
Vol. 42, No. 2, pp. A797–A821

ASYMPTOTICALLY EXACT A POSTERIORI ERROR ESTIMATES OF EIGENVALUES BY THE CROUZEIX–RAVIART ELEMENT AND ENRICHED CROUZEIX–RAVIART ELEMENT*

JUN HU† AND LIMIN MA†

Abstract. Two asymptotically exact a posteriori error estimates are proposed for eigenvalues by the nonconforming Crouzeix–Raviart and enriched Crouzeix–Raviart elements. The main challenge in the design of such error estimators comes from the nonconformity of the finite element spaces used. Such nonconformity causes two difficulties: the first is the construction of high accuracy gradient recovery algorithms, and the second is a computable high accuracy approximation of a consistency error term. The first difficulty was solved for both nonconforming elements in a previous paper. Two methods are proposed to solve the second difficulty in the present paper. In particular, this solution allows the use of high accuracy gradient recovery techniques. Further, a postprocessing algorithm is designed by utilizing asymptotically exact a posteriori error estimators to construct the weights of a combination of two approximate eigenvalues. This algorithm requires solving only one eigenvalue problem and admits high accuracy eigenvalue approximations both theoretically and numerically.

Key words. eigenvalue problems, nonconforming elements, asymptotically exact a posteriori error estimates

AMS subject classifications. 65N30, 73C02

DOI. 10.1137/19M1261997

1. Introduction.

Asymptotically exact a posteriori error estimates are widely used to improve accuracy of approximations. A posteriori error estimates were first proposed by Babuška and Rheinboldt in 1978 [2]. Since then, some important branches of a posteriori error estimates have been developed, such as residual type a posteriori error estimates [1, 4, 7, 8] and recovery type a posteriori error estimates [3, 6, 23, 32, 34, 35]. For eigenvalues of the Laplacian operator by the conforming linear element, asymptotically exact a posteriori error estimates were proposed and analyzed in [26]. These error estimates play an important role in improving the accuracy of eigenvalues to a remarkable fourth order. For that conforming element, the error in the eigenvalues can be decomposed into the energy norm of the error in the approximation of the eigenfunctions and a higher order term. Asymptotically exact a posteriori error estimates follow directly from this crucial fact and an application of high accuracy gradient recovery techniques, such as polynomial preserving recovery techniques (PPR) in [11, 25], Zienkiewicz–Zhu superconvergence patch recovery techniques in [36], and superconvergent cluster recovery methods in [19].

As for nonconforming elements, the error for the eigenvalues is composed of the energy norm of the error in the approximation of the corresponding eigenfunctions, an extra consistency error term and a higher order term. The nonconformity causes two major difficulties: the first is the construction of high accuracy gradient recovery algorithms, and the second is a computable high accuracy approximation of the consistency error term. A previous paper [16] analyzed an optimal superconvergence result for both the nonconforming Crouzeix–Raviart (CR) element and the enriched

*Submitted to the journal's Methods and Algorithms for Scientific Computing section May 17, 2019; accepted for publication (in revised form) December 23, 2019; published electronically March 23, 2020.

https://doi.org/10.1137/19M1261997

Funding: This work was supported by NSFC projects 11625101, 91430213, and 11421101.

†LMAM and School of Mathematical Sciences, Peking University, Beijing 100871, People's Republic of China (hujun@math.pku.edu.cn, maliminpku@gmail.com).

Crouzeix–Raviart (ECR) element. It offers a computable high accuracy approximation to the gradient of the eigenfunctions. The aforementioned consistency error term requires approximating the eigenfunctions themselves with high accuracy, not the gradient of the eigenfunctions. The fact that there exist no such high accuracy function recovery techniques in the literature causes the second difficulty for nonconforming elements.

Two types of asymptotically exact a posteriori error estimates for the eigenvalues are designed for the nonconforming CR element and the ECR element. The main idea here is to turn this function recovery problem into a high accuracy gradient recovery problem. The first type of a posteriori error estimate employs a commuting interpolation of eigenfunctions, and the second type makes use of a conforming interpolation of eigenfunctions. Both types of asymptotically exact a posteriori error estimates require a high accuracy gradient recovery technique for the nonconforming CR element and the ECR element. The first design of asymptotically exact a posteriori error estimates is much easier to implement but requires a commuting interpolation, while the other applies for more general nonconforming elements as long as the corresponding discrete space contains a conforming subspace. Although both error estimates achieve the same predicted accuracy, experiments indicate even higher accuracy for the first type of error estimates when the eigenfunctions are smooth enough, while the second type admits much better experimental performance when the eigenfunctions are singular.

An additional technique for high precision eigenvalues is to combine two approximate eigenvalues by a weighted-average [13]. The accuracy of the resulting combined eigenvalues depends on the accuracy of the weights. In [13], two finite elements are employed to solve eigenvalue problems on two meshes, with one element producing upper bounds of the eigenvalues and the other producing lower bounds. The main idea there is to design approximate weights through these four resulting discrete eigenvalues. In experiments, this algorithm is observed to be quite efficient.

By use of the aforementioned asymptotically exact a posteriori error estimates, a new postprocessing algorithm is proposed and analyzed to improve the accuracy of the approximate eigenvalues. Given lower bounds of the eigenvalues and the corresponding nonconforming approximate eigenfunctions, an application of the average-projection method [14] to these eigenfunctions yields conforming approximate eigenfunctions. By [14], Rayleigh quotients of such conforming eigenfunctions are asymptotic upper bounds of the eigenvalues. The new algorithm combines the lower and upper bounds of the eigenvalues by a weighted-average. The weights here are designed from the corresponding asymptotically exact a posteriori error estimates. The resulting combined eigenvalues are proved to admit higher accuracy both theoretically and experimentally. It needs to be pointed out that only one discrete eigenvalue problem needs to be solved in this new algorithm.

The remainder of the paper is organized as follows. Section 2 presents second order elliptic eigenvalue problems and some notation. Section 3 establishes and analyzes asymptotically exact a posteriori error estimates for eigenvalues by the nonconforming CR element and the ECR element. Section 4 proposes two postprocessing algorithms to approximate eigenvalues with high accuracy. Section 5 presents some numerical tests.

2. Notation and preliminaries.

2.1. Notation. We first introduce some basic notation. Given a nonnegative integer k and a bounded domain $\Omega \subset \mathbb{R}^2$ with Lipschitz boundary $\partial\Omega$, let $H^k(\Omega, \mathbb{R})$,

$\|\cdot\|_{k,\Omega}$, and $|\cdot|_{k,\Omega}$ denote the usual Sobolev spaces, norm, and seminorm, respectively. Denote the standard $L^2(\Omega,\mathbb{R})$ inner product and $L^2(K,\mathbb{R})$ inner product by $(\cdot,\cdot)$ and $(\cdot,\cdot)_{0,K}$, respectively. Let $H_0^1(\Omega,\mathbb{R}) = \{u \in H^1(\Omega,\mathbb{R}) : u|_{\partial\Omega} = 0\}$.

Suppose that $\Omega \subset \mathbb{R}^2$ is a bounded polygonal domain covered exactly by a shape-regular partition $\mathcal{T}_h$ of simplices. Let element K have vertices $\mathbf{p}_i = (p_{i1}, p_{i2}), 1 \le i \le 3$, oriented counterclockwise, and corresponding barycentric coordinates $\{\phi_i\}_{i=1}^3$. Denote by $\{e_i\}_{i=1}^3$ the edges of element K and by $\{\mathbf{t}_i\}_{i=1}^3$ the unit tangent vectors with counterclockwise orientation. Denote the column vectors by $\mathbf{e}_1 = (1,0)^T$ and $\mathbf{e}_2 = (0,1)^T$.

Let $|K|$ denote the volume of element K and $|e|$ denote the length of edge e. Let h_K denote the diameter of element $K \in \mathcal{T}_h$, and let $h = \max_{K\in\mathcal{T}_h} h_K$. Denote the set of all interior edges and boundary edges of $\mathcal{T}_h$ by $\mathcal{E}_h^i$ and $\mathcal{E}_h^b$, respectively, and let $\mathcal{E}_h = \mathcal{E}_h^i \cup \mathcal{E}_h^b$. For any interior edge $e = K_e^1 \cap K_e^2$, we denote the element with larger global label by K_e^1, and the element with smaller global label by K_e^2. Let $\{\cdot\}$ and $[\cdot]$ be the average and jump of piecewise functions over edge e, namely,

$$\{v\}|_e := \frac{1}{2}(v|_{K_e^1} + v|_{K_e^2}), \qquad [v]|_e := v|_{K_e^1} - v|_{K_e^2},$$

for any piecewise function v. For $K \subset \mathbb{R}^2$, $r \in \mathbb{Z}^+$, let $P_r(K)$ be the space of all polynomials of degree not greater than r on K. Denote the second order derivatives $\frac{\partial^2 u}{\partial x_i \partial x_j}$ by $\partial_{x_i x_j} u$, $1 \le i,j \le 2$, and denote the piecewise gradient operator and the piecewise Hessian operator by ∇_h and ∇_h^2, respectively.

Throughout the paper, a positive constant independent of the mesh size is denoted by C, which refers to different values at different places.

2.2. Nonconforming elements for eigenvalue problems. We consider a model eigenvalue problem of finding $(\lambda, u) \in \mathbb{R} \times V$ such that $\| u \|_{0,\Omega} = 1$ and

$$a(u,v) = \lambda(u,v) \quad \text{for any } v \in V, \tag{2.1}$$

where $V := H_0^1(\Omega,\mathbb{R})$. The bilinear form $a(w,v) := \int_\Omega \nabla w \cdot \nabla v \, dx$ is symmetric, bounded, and coercive, namely, for any $w, v \in V$,

$$a(w,v) = a(v,w), \quad |a(w,v)| \le C \| w \|_{1,\Omega} \| v \|_{1,\Omega}, \quad \| v \|_{1,\Omega}^2 \le C a(v,v).$$

The eigenvalue problem (2.1) has a sequence of eigenvalues

$$0 < \lambda_1 \le \lambda_2 \le \lambda_3 \le \cdots \nearrow +\infty,$$

and the corresponding eigenfunctions $u_1, u_2, u_3, \ldots$, with

$$(u_i, u_j) = \delta_{ij} \ \text{ with } \delta_{ij} = \begin{cases} 0, & i \ne j, \\ 1, & i = j. \end{cases}$$

Let V_h be a nonconforming finite element approximation of V over $\mathcal{T}_h$. The corresponding finite element approximation of (2.1) is to find $(\lambda_h, u_h) \in \mathbb{R} \times V_h$ such that $\| u_h \|_{0,\Omega} = 1$ and

$$a_h(u_h, v_h) = \lambda_h(u_h, v_h) \quad \text{for any } v_h \in V_h, \tag{2.2}$$

with the discrete bilinear form $a_h(w_h, v_h)$ defined elementwise as

$$a_h(w_h, v_h) := \sum_{K\in\mathcal{T}_h} \int_K \nabla_h w_h \cdot \nabla_h v_h \, dx.$$

Let $N = \dim V_h$. Suppose that $\|\cdot\|_h := a_h(\cdot,\cdot)^{1/2}$ is a norm over the discrete space V_h, the discrete problem (2.2) admits a sequence of discrete eigenvalues

$$0 < \lambda_{1,h} \le \lambda_{2,h} \le \lambda_{3,h} \le \cdots \le \lambda_{N,h},$$

and the corresponding eigenfunctions $u_{1,h}, u_{2,h}, \ldots, u_{N,h}$ with $(u_{i,h}, u_{j,h}) = \delta_{ij}$.

We consider the following two nonconforming elements, i.e., the CR element and the ECR element:

- The CR element space over $\mathcal{T}_h$ is defined in [9] by

$$V_{\mathrm{CR}} := \Big\{ v \in L^2(\Omega,\mathbb{R}) \big| v|_K \in P_1(K) \text{ for any } K \in \mathcal{T}_h, \int_e [v]\, ds = 0 \text{ for any } e \in \mathcal{E}_h^i, \int_e v\, ds = 0 \text{ for any } e \in \mathcal{E}_h^b \Big\}.$$

Moreover, we define the canonical interpolation operator $\Pi_{\mathrm{CR}} : H_0^1(\Omega,\mathbb{R}) \to V_{\mathrm{CR}}$ as follows:

$$\int_e \Pi_{\mathrm{CR}} v\, ds = \int_e v\, ds \quad \text{for any } e \in \mathcal{E}_h,\ v \in H_0^1(\Omega,\mathbb{R}). \tag{2.3}$$

Denote the approximate eigenpair of (2.2) in the nonconforming space V_{CR} by $(\lambda_{\mathrm{CR}}, u_{\mathrm{CR}})$ with $\| u_{\mathrm{CR}} \|_{0,\Omega} = 1$.

- The ECR element space over $\mathcal{T}_h$ is defined in [12] by

$$V_{\mathrm{ECR}} := \Big\{ v \in L^2(\Omega,\mathbb{R}) \big| v|_K \in \mathrm{ECR}(K) \text{ for any } K \in \mathcal{T}_h, \int_e [v]\, ds = 0 \text{ for any } e \in \mathcal{E}_h^i, \int_e v\, ds = 0 \text{ for any } e \in \mathcal{E}_h^b \Big\},$$

with $\mathrm{ECR}(K) = P_1(K) + \mathrm{span}\{x_1^2 + x_2^2\}$. Define the canonical interpolation operator $\Pi_{\mathrm{ECR}} : H_0^1(\Omega,\mathbb{R}) \to V_{\mathrm{ECR}}$ by

$$\int_e \Pi_{\mathrm{ECR}} v\, ds = \int_e v\, ds, \quad \int_K \Pi_{\mathrm{ECR}} v\, dx = \int_K v\, dx \quad \forall e \in \mathcal{E}_h, K \in \mathcal{T}_h. \tag{2.4}$$

Denote the approximate eigenpair of (2.2) in the nonconforming space V_{ECR} by $(\lambda_{\mathrm{ECR}}, u_{\mathrm{ECR}})$ with $\| u_{\mathrm{ECR}} \|_{0,\Omega} = 1$.

It follows from the theory of nonconforming approximations of eigenvalue problems in [12, 27] that

$$|\lambda - \lambda_{\mathrm{CR}}| + \| u - u_{\mathrm{CR}} \|_{0,\Omega} + h^s \| \nabla_h (u - u_{\mathrm{CR}}) \|_{0,\Omega} \le C h^{2s} \| u \|_{1+s,\Omega}, \tag{2.5}$$

$$|\lambda - \lambda_{\mathrm{ECR}}| + \| u - u_{\mathrm{ECR}} \|_{0,\Omega} + h^s \| \nabla_h (u - u_{\mathrm{ECR}}) \|_{0,\Omega} \le C h^{2s} \| u \|_{1+s,\Omega}, \tag{2.6}$$

provided that $u \in H^{1+s}(\Omega,\mathbb{R}) \cap H_0^1(\Omega,\mathbb{R})$, $0 < s \le 1$.

For the CR element and the ECR element, the following commuting property of the canonical interpolations holds:

$$\begin{aligned} &\int_K \nabla(w - \Pi_{\mathrm{CR}} w) \cdot \nabla v_h\, dx = 0 \quad \text{for any } w \in V, v_h \in V_{\mathrm{CR}}, \\ &\int_K \nabla(w - \Pi_{\mathrm{ECR}} w) \cdot \nabla v_h\, dx = 0 \quad \text{for any } w \in V, v_h \in V_{\mathrm{ECR}}; \end{aligned} \tag{2.7}$$

see [9, 12] for details.

2.3. Some Taylor expansions. On each element K, denote the centroid of element K by $\mathbf{M}_K = (M_1, M_2)$. Let $A_K = \sum_{i,j=1,i\neq j}^{3} \big((p_{i1}-p_{j1})^2 - (p_{i2}-p_{j2})^2\big)$, $B_K = \sum_{i=1}^{3} \big(2p_{i1}p_{i2} - \sum_{j=1,j\neq i}^{3} p_{i1}p_{j2}\big)$, and $H_K = \sum_{i=1}^{3} |e_i|^2$. We introduce three shorthand notations,

$$\phi^1_{\mathrm{ECR}}(\mathbf{x}) = (x_1-M_1)^2 - (x_2-M_2)^2, \qquad \phi^2_{\mathrm{ECR}}(\mathbf{x}) = (x_1-M_1)(x_2-M_2),$$
$$\phi^3_{\mathrm{ECR}}(\mathbf{x}) = 2 - \frac{36}{H_K}\sum_{i=1}^{2}(x_i-M_i)^2.$$

Note that $P_2(K) = P_1(K) + \mathrm{span}\{\phi^1_{\mathrm{ECR}}, \phi^2_{\mathrm{ECR}}, \phi^3_{\mathrm{ECR}}\}$.

For any element K and $H_h \in P_0(K, \mathbb{R}^{2\times 2})$, define the quadratic polynomials

$$\begin{aligned}
P^K_{\mathrm{P}_1}(H_h) =& -\frac{1}{2}\sum_{i=1}^{3} \mathbf{t}_i^T H_h \mathbf{t}_i |e_i|^2 \phi_{i+1}\phi_{i-1},\\
P^K_{\mathrm{CR}}(H_h) =& \frac{\mathbf{e}_1^T H_h \mathbf{e}_1 - \mathbf{e}_2^T H_h \mathbf{e}_2}{4}(I-\Pi_{\mathrm{ECR}})\phi^1_{\mathrm{ECR}} + \mathbf{e}_1^T H_h \mathbf{e}_2 (I-\Pi_{\mathrm{ECR}})\phi^2_{\mathrm{ECR}}\\
&- \left(\frac{A_K+H_K}{144}\mathbf{e}_1^T H_h \mathbf{e}_1 + \frac{H_K-A_K}{144}\mathbf{e}_2^T H_h \mathbf{e}_2 + \frac{B_K}{36}\mathbf{e}_1^T H_h \mathbf{e}_2\right)\phi^3_{\mathrm{ECR}},\\
P^K_{\mathrm{ECR}}(H_h) =& \frac{\mathbf{e}_1^T H_h \mathbf{e}_1 - \mathbf{e}_2^T H_h \mathbf{e}_2}{4}(I-\Pi_{\mathrm{ECR}})\phi^1_{\mathrm{ECR}} + \mathbf{e}_1^T H_h \mathbf{e}_2 (I-\Pi_{\mathrm{ECR}})\phi^2_{\mathrm{ECR}},
\end{aligned} \tag{2.8}$$

where ϕ_i is the corresponding barycentric coordinate to vertex $\mathbf{p}_i$.

The following lemma lists the Taylor expansion of the canonical interpolation error for the conforming linear element, the CR element, and the ECR element, respectively. See [15, 18] for more details.

LEMMA 2.1. *For any quadratic function $w \in P_2(K)$,*

$$\begin{aligned}
(I-\Pi_{\mathrm{P}_1})w =& \quad P^K_{\mathrm{P}_1}(\nabla^2 w),\\
(I-\Pi_{\mathrm{CR}})w =& \quad P^K_{\mathrm{CR}}(\nabla^2 w),\\
(I-\Pi_{\mathrm{ECR}})w =& \quad P^K_{\mathrm{ECR}}(\nabla^2 w).
\end{aligned} \tag{2.9}$$

2.4. Superconvergence results for the CR element. Before designing a posteriori error estimates, we represent the postprocessing mechanism, which was first proposed in [5] and then analyzed in [17] for the CR element. The shape function space of the Raviart–Thomas element [28] reads

$$\mathrm{RT}_K := (P_0(K))^2 + \mathbf{x}P_0(K) \quad \text{for any } K \in \mathcal{T}_h,$$

and the corresponding finite element space is

$$\mathrm{RT}(\mathcal{T}_h) := \big\{\tau \in H(\mathrm{div}, \Omega, \mathbb{R}^2) : \tau|_K \in \mathrm{RT}_K \text{ for any } K \in \mathcal{T}_h\big\}.$$

Given $\boldsymbol{q} \in \mathrm{RT}(\mathcal{T}_{\mathrm{h}})$, define function $K_h\boldsymbol{q}|_K \in P_1(K)\times P_1(K)$ as in [5, 17].

DEFINITION 2.1. (1) *For each interior edge $e \in \mathcal{E}_h^i$, the elements K_e^1 and K_e^2 are the pair of elements sharing e. Then the value of $K_h\boldsymbol{q}$ at the midpoint $\boldsymbol{m}_e$ of e is*

$$K_h\boldsymbol{q}(\boldsymbol{m}_e) = \frac{1}{2}(\boldsymbol{q}|_{K_e^1}(\boldsymbol{m}_e) + \boldsymbol{q}|_{K_e^2}(\boldsymbol{m}_e)).$$

(2) *For each boundary edge $e \in \mathcal{E}_h^b$, let K be the element having e as an edge, and let K' be an element sharing an edge $e' \in \mathcal{E}_h^i$ with K. Let e'' denote the edge of K'*

that does not intersect with e, and let $\boldsymbol{m}$, $\boldsymbol{m}'$, *and* $\boldsymbol{m}''$ *be the midpoints of the edges* e, e', *and* e'', *respectively. Then the value of* $K_h\boldsymbol{q}$ *at the point* $\boldsymbol{m}$ *is*

$$K_h\boldsymbol{q}(\boldsymbol{m}) = 2K_h\boldsymbol{q}(\boldsymbol{m}') - K_h\boldsymbol{q}(\boldsymbol{m}'').$$

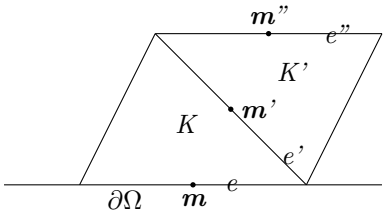

The CR element solution for source problems admits a first order superconvergence on uniform triangulations [16]. According to [15], the eigenfunction $u_{\rm CR}$ superconverges to the CR element solution for the corresponding source problem. These two facts lead to the superconvergence result

$$\| \nabla u - K_h\nabla_h u_{\rm CR} \|_{0,\Omega} \leq Ch^2|\ln h|^{1/2}|u|_{\frac{7}{2},\Omega}, \tag{2.10}$$

provided that $u \in H^{\frac{7}{2}}(\Omega,\mathbb{R}) \cap H_0^1(\Omega,\mathbb{R})$. A similar order superconvergence result of the CR element on a mildly structured mesh with a somehow higher regularity assumption was analyzed in [22] for source problems, which can be extended to eigenvalue problems. This superconvergence property (2.10) leads to the following lemma for second order derivatives of eigenfunctions.

LEMMA 2.2. *Let* (λ, u) *be an eigenpair of* (2.1) *with* $u \in H^{\frac{7}{2}}(\Omega,\mathbb{R}) \cap H_0^1(\Omega,\mathbb{R})$, *and let* $(\lambda_{\rm CR}, u_{\rm CR})$ *be the corresponding approximate eigenpair of* (2.2) *in* $V_{\rm CR}$. *It holds that*

$$\| \nabla^2 u - \nabla_h K_h \nabla_h u_{\rm CR} \|_{0,\Omega} \leq Ch|\ln h|^{1/2}|u|_{\frac{7}{2},\Omega},$$

provided that $u \in H^{\frac{7}{2}}(\Omega,\mathbb{R}) \cap H_0^1(\Omega,\mathbb{R})$.

Proof. Let $\Pi_{\rm P_2}$ be the second order Lagrange interpolation; namely, the interpolation $\Pi_{\rm P_2}u$ is a piecewise quadratic function over $\mathcal{T}_h$ and admits the same value as u at the vertices of each element and the midpoint of each edge. It follows from the theory in [29] that

$$\left|u - \Pi_{\rm P_2}u\right|_{i,\Omega} \leq Ch^{3-i}|u|_{3,\Omega},\ 0 \leq i \leq 2. \tag{2.11}$$

Due to the triangle inequality,

$$\| \nabla^2 u - \nabla_h K_h \nabla_h u_{\rm CR} \|_{0,\Omega} \leq \| \nabla^2 u - \nabla_h^2 \Pi_{\rm P_2} u \|_{0,\Omega} + \| \nabla_h^2 \Pi_{\rm P_2} u - \nabla_h K_h \nabla_h u_{\rm CR} \|_{0,\Omega}\,. \tag{2.12}$$

By the inverse inequality,

$$\| \nabla_h^2 \Pi_{\rm P_2} u - \nabla_h K_h \nabla_h u_{\rm CR} \|_{0,\Omega} \leq Ch^{-1} \| \nabla_h \Pi_{\rm P_2} u - K_h \nabla_h u_{\rm CR} \|_{0,\Omega}\,. \tag{2.13}$$

A combination of (2.10), (2.11), and (2.13) yields

$$\begin{aligned} &\| \nabla_h^2 \Pi_{\rm P_2} u - \nabla_h K_h \nabla_h u_{\rm CR} \|_{0,\Omega} \\ &\quad \leq\ Ch^{-1}|\Pi_{\rm P_2}u - u|_{1,\Omega} + h^{-1} \| \nabla u - K_h \nabla_h u_{\rm CR} \|_{0,\Omega} \leq Ch|\ln h|^{1/2}|u|_{\frac{7}{2},\Omega}. \end{aligned} \tag{2.14}$$

A substitution of (2.11) and (2.14) into (2.12) concludes that

$$\| \nabla^2 u - \nabla_h K_h \nabla_h u_{\rm CR} \|_{0,\Omega} \leq Ch |\ln h|^{1/2} |u|_{\frac{7}{2},\Omega},$$

which completes the proof. ∎

3. Asymptotically exact a posteriori error estimates. In this section, asymptotically exact a posteriori error estimates for eigenvalues are designed and analyzed for the CR element and the ECR element.

For eigenvalues of the Laplacian operator solved by the conforming linear element, asymptotically exact a posteriori error estimates in [26] are based on a simple identity

$$\lambda_h - \lambda = |u - u_h|^2_{1,\Omega} - \lambda \| u - u_h \|^2_{0,\Omega},$$

where (λ_h, u_h) is an approximate eigenpair by this conforming element. The L^2 norm of the error in the approximation of eigenfunctions is of higher order compared to their energy norm. By approximating the first term $|u - u_h|^2_{1,\Omega}$ with high accuracy gradient recovery techniques in [19, 25, 36], asymptotically exact a posteriori error estimates for eigenvalues result following the above identity.

For nonconforming elements of second order elliptic eigenvalue problems, there exists an identity similar to the one in [33].

LEMMA 3.1. *Let (λ, u) be an eigenpair of (2.1), and let (λ_h, u_h) be the corresponding approximate eigenpair of (2.2). There holds*

$$\lambda - \lambda_h = |u - u_h|^2_{1,h} + 2(a_h(u, u_h) - \lambda_h(u, u_h)) - \lambda_h \|u - u_h\|^2_{0,\Omega}. \tag{3.1}$$

Proof. By (2.1) and (2.2),

$$a_h(u - u_h, u - u_h) = a(u, u) + a_h(u_h, u_h) - 2a_h(u, u_h) = \lambda + \lambda_h - 2a_h(u, u_h).$$

It follows that

$$\lambda - \lambda_h = a_h(u - u_h, u - u_h) + 2a_h(u, u_h) - 2\lambda_h. \tag{3.2}$$

Note that $\|u - u_h\|^2_{0,\Omega} + 2(u, u_h) = 2$. The identity (3.2) reads

$$\lambda - \lambda_h = a_h(u - u_h, u - u_h) + 2(a_h(u, u_h) - \lambda_h(u, u_h)) - \lambda_h \|u - u_h\|^2_{0,\Omega},$$

which completes the proof. ∎

Compared to the identity for conforming elements, the identity (3.1) includes an extra term, $a_h(u, u_h) - \lambda_h(u, u_h)$. The nonconformity leads to this consistency error term, which relates to values of the eigenfunctions. Since there are no high accuracy techniques in the literature to recover eigenfunctions themselves, this extra term causes the difficulty of approximating discrete eigenvalues with high accuracy.

3.1. First type of asymptotically exact a posteriori error estimates. For both the CR element and the ECR element, the canonical interpolation admits a commuting property (2.7). By subtracting (2.7) from the extra term, the aforementioned consistency error can be expressed in terms of the interpolation error. Taylor expansions in Lemma 2.1 imply that the dominant ingredients of the interpolation error are the second order derivatives of the eigenfunctions. This important property turns the function recovery problem into a gradient recovery problem. To be specific, for the

CR element, thanks to the commuting property (2.7) of the canonical interpolation operator $\Pi_{\rm CR}$,

$$\lambda - \lambda_{\rm CR} = |u - u_{\rm CR}|_{1,h}^2 - 2\lambda_{\rm CR}(u - \Pi_{\rm CR}u, u_{\rm CR}) - \lambda_{\rm CR}\|u - u_{\rm CR}\|_{0,\Omega}^2. \tag{3.3}$$

The term $|u-u_{\rm CR}|_{1,h}^2$ can be approximated with high accuracy by a direct application of gradient recovery techniques [19, 25, 36] or superconvergent results in [16, 22]. By the Taylor expansions in Lemma 2.1 and the superconvergent result in Lemma 2.2, the interpolation error term $(u-\Pi_{\rm CR}u, u_{\rm CR})$ can be approximated with high accuracy by the use of these gradient recovery techniques. Then, asymptotically exact a posteriori error estimates for eigenvalues are designed from the identity (3.3). This idea also works for eigenvalues by the ECR element.

Note that within each element K, both $\nabla_h K_h \nabla_h u_{\rm CR}$ and $\nabla_h K_h \nabla_h u_{\rm ECR}$ belong to $P_0(K, \mathbb{R}^{2\times 2})$. Define the a posteriori error estimates

$$F_{\rm CR,1}^{\rm CR} = \| K_h\nabla_h u_{\rm CR} - \nabla_h u_{\rm CR}\|_{0,\Omega}^2 - 2\lambda_{\rm CR}\sum_{K\in\mathcal{T}_h}\int_K P_{\rm CR}^K(\nabla_h K_h\nabla_h u_{\rm CR})u_{\rm CR}\,dx, \tag{3.4}$$

$$F_{\rm ECR,1}^{\rm ECR} = \| K_h\nabla_h u_{\rm ECR} - \nabla_h u_{\rm ECR}\|_{0,\Omega}^2 - 2\lambda_{\rm ECR}\sum_{K\in\mathcal{T}_h}\int_K P_{\rm ECR}^K(\nabla_h K_h\nabla_h u_{\rm ECR})u_{\rm ECR}\,dx \tag{3.5}$$

with the polynomials $P_{\rm CR}^K$ and $P_{\rm ECR}^K$ defined in (2.8).

Let $\Pi_{\rm M}$ be the interpolation of the Morley element in [24] with

$$\Pi_{\rm M} v(\mathbf{p}_i) = v(\mathbf{p}_i), \quad \int_{e_i}\frac{\partial \Pi_{\rm M} v}{\partial \mathbf{n}}\,ds = \int_{e_i}\frac{\partial v}{\partial \mathbf{n}}\,ds, \quad 1\le i\le 3.$$

It holds that

$$\int_K \nabla^2(I-\Pi_{\rm M})v\,dx = 0 \quad \text{and} \quad |(I-\Pi_{\rm M})v|_{i,K} \le Ch^{3-i}|v|_{3,K} \quad \forall\ 0\le i\le 2. \tag{3.6}$$

THEOREM 3.1. *Let (λ, u) be an eigenpair of (2.1) with $u\in H^{\frac{7}{2}}(\Omega,\mathbb{R})\cap H_0^1(\Omega,\mathbb{R})$, and let $(\lambda_{\rm CR}, u_{\rm CR})$ be the corresponding approximate eigenpair of (2.2) in $V_{\rm CR}$. The a posteriori error estimate $F_{\rm CR,1}^{\rm CR}$ in (3.4) satisfies*

$$\left|\lambda - \lambda_{\rm CR} - F_{\rm CR,1}^{\rm CR}\right| \le Ch^3|\ln h|^{1/2}|u|_{\frac{7}{2},\Omega}^2.$$

Proof. By the definition of $F_{\rm CR,1}^{\rm CR}$ in (3.4) and (3.3),

$$\begin{aligned}\lambda - \lambda_{\rm CR} - F_{\rm CR,1}^{\rm CR} = {} & |u-u_{\rm CR}|_{1,h}^2 - \| K_h\nabla_h u_{\rm CR} - \nabla_h u_{\rm CR}\|_{0,\Omega}^2 - \lambda_{\rm CR}\|u-u_{\rm CR}\|_{0,\Omega}^2 \\ & - 2\lambda_{\rm CR}\sum_{K\in\mathcal{T}_h}\left(u - \Pi_{\rm CR}u - P_{\rm CR}^K(\nabla_h^2\Pi_{\rm M}u), u_{\rm CR}\right)_{0,K} \\ & - 2\lambda_{\rm CR}\sum_{K\in\mathcal{T}_h}\left(P_{\rm CR}^K(\nabla_h^2\Pi_{\rm M}u) - P_{\rm CR}^K(\nabla_h K_h\nabla_h u_{\rm CR}), u_{\rm CR}\right)_{0,K}.\end{aligned} \tag{3.7}$$

Thanks to (2.5) and (2.10),

$$\left||u-u_{\rm CR}|_{1,h}^2 - \| K_h\nabla_h u_{\rm CR} - \nabla_h u_{\rm CR}\|_{0,\Omega}^2\right| \le Ch^3|\ln h|^{1/2}|u|_{\frac{7}{2},\Omega}^2. \tag{3.8}$$

According to Lemma 2.1,

$$(I-\Pi_{\rm CR})\Pi_{\rm M}u = P_{\rm CR}^K(\nabla_h^2\Pi_{\rm M}u).$$

Thus, it follows from (3.6) that

$$\|u - \Pi_{\mathrm{CR}} u - P_{\mathrm{CR}}^K(\nabla_h^2 \Pi_{\mathrm{M}} u)\|_{0,K} = \|(I - \Pi_{\mathrm{CR}})(I - \Pi_{\mathrm{M}})u\|_{0,K} \le Ch^3 |u|_{3,K}. \tag{3.9}$$

Since $P_{\mathrm{CR}}^K(H_h)$ is a linear function of H_h,

$$\begin{aligned} &\Big| \sum_{K \in \mathcal{T}_h} \big(P_{\mathrm{CR}}^K(\nabla_h^2 \Pi_{\mathrm{M}} u) - P_{\mathrm{CR}}^K(\nabla_h K_h \nabla_h u_{\mathrm{CR}}), u_{\mathrm{CR}}\big)_{0,K} \Big| \\ &\le \sum_{K \in \mathcal{T}_h} \|P_{\mathrm{CR}}^K(\nabla_h^2 \Pi_{\mathrm{M}} u - \nabla_h K_h \nabla_h u_{\mathrm{CR}})\|_{0,K} \|u_{\mathrm{CR}}\|_{0,K}. \end{aligned} \tag{3.10}$$

According to Lemma 2.1 and the Bramble–Hilbert lemma,

$$\|P_{\mathrm{CR}}^K(H_h)\|_{0,K} \le Ch^2 \|H_h\|_{0,K}.$$

Let $H_h = \nabla_h^2 \Pi_{\mathrm{M}} u - \nabla_h K_h \nabla_h u_{\mathrm{CR}}$. Thus,

$$\|P_{\mathrm{CR}}^K(\nabla_h^2 \Pi_{\mathrm{M}} u - \nabla_h K_h \nabla_h u_{\mathrm{CR}})\|_{0,K} \le Ch^2 \|\nabla_h^2 \Pi_{\mathrm{M}} u - \nabla_h K_h \nabla_h u_{\mathrm{CR}}\|_{0,K}. \tag{3.11}$$

Thanks to (3.6) and Lemma 2.2,

$$\begin{aligned} \|\nabla_h^2 \Pi_{\mathrm{M}} u - \nabla_h K_h \nabla_h u_{\mathrm{CR}}\|_{0,K} &\le \|\nabla_h^2 \Pi_{\mathrm{M}} u - \nabla^2 u\|_{0,K} + \|\nabla^2 u - \nabla_h K_h \nabla_h u_{\mathrm{CR}}\|_{0,K} \\ &\le Ch |\ln h|^{1/2} |u|_{\frac{7}{2},\Omega}. \end{aligned} \tag{3.12}$$

A combination of (3.10), (3.11), and (3.12) leads to

$$\Big| \sum_{K \in \mathcal{T}_h} \big(P_{\mathrm{CR}}^K(\nabla_h^2 \Pi_{\mathrm{M}} u) - P_{\mathrm{CR}}^K(\nabla_h K_h \nabla_h u_{\mathrm{CR}}), u_{\mathrm{CR}}\big)_{0,K} \Big| \le Ch^3 |\ln h|^{1/2} |u|_{\frac{7}{2},\Omega}^2. \tag{3.13}$$

A substitution of (2.5), (3.8), (3.9), and (3.13) into (3.7) concludes that

$$\big|\lambda - \lambda_{\mathrm{CR}} - F_{\mathrm{CR},1}^{\mathrm{CR}}\big| \le Ch^3 |\ln h|^{1/2} |u|_{\frac{7}{2},\Omega}^2$$

and completes the proof. ∎

Compared to the terms in (3.3), the above analysis shows that the term $\| K_h \nabla_h u_{\mathrm{CR}} - \nabla_h u_{\mathrm{CR}} \|_{0,\Omega}^2$ in $F_{\mathrm{CR},1}^{\mathrm{CR}}$ approximates $|u - u_{\mathrm{CR}}|_{1,h}^2$ with high accuracy, and $\sum_{K \in \mathcal{T}_h} \int_K P_{\mathrm{CR}}^K(\nabla_h K_h \nabla_h u_{\mathrm{CR}}) u_{\mathrm{CR}}\, dx$ approximates $(u - \Pi_{\mathrm{CR}} u, u_{\mathrm{CR}})$ with high accuracy. Notice that other a posteriori error estimates can be constructed following (3.4) with different recovered gradients from $K_h \nabla_h u_{\mathrm{CR}}$. The resulting a posteriori error estimates are asymptotically exact as long as the recovered gradient admits a superconvergence result.

Similarly, the a posteriori error estimate $F_{\mathrm{ECR},1}^{\mathrm{ECR}}$ in (3.5) is also asymptotically exact as presented in the following theorem.

THEOREM 3.2. *Let (λ, u) be an eigenpair of (2.1) with $u \in H^{\frac{7}{2}}(\Omega, \mathbb{R}) \cap H_0^1(\Omega, \mathbb{R})$, and let $(\lambda_{\mathrm{ECR}}, u_{\mathrm{ECR}})$ be the corresponding approximate eigenpair of (2.2) in V_{ECR}. Then,*

$$\big|\lambda - \lambda_{\mathrm{ECR}} - F_{\mathrm{ECR},1}^{\mathrm{ECR}}\big| \le Ch^3 |\ln h|^{1/2} |u|_{\frac{7}{2},\Omega}^2.$$

Remark 3.1. Suppose that (λ, u) is an eigenpair of the biharmonic operator with $u \in H^{\frac{9}{2}}(\Omega, \mathbb{R}) \cap H_0^2(\Omega, \mathbb{R})$, and that $(\lambda_{\mathrm{M}}, u_{\mathrm{M}})$ is the corresponding approximate eigenpair by the Morley element on a uniform triangulation $\mathcal{T}_h$. Thanks to the superconvergence of the Hellan–Herrmann–Johnson element and its equivalence to the Morley element, the recovered Hessian $K_h \nabla_h^2 u_{\mathrm{M}}$ superconverges to $\nabla^2 u$. Since the canonical interpolation operator of the Morley element also admits the commuting property, a similar procedure produces asymptotically exact a posteriori error estimates for eigenvalues by the Morley element.

3.2. Second type of asymptotically exact a posteriori error estimates. The second type of asymptotically exact a posteriori error estimates works for any nonconforming elements as long as the corresponding discrete space contains a conforming subspace and there exists some high accuracy gradient recovery technique for the elements.

The canonical interpolation of a conforming element is employed here to approximate the consistency error term. Take the CR element, for example,

$$\begin{aligned} \lambda - \lambda_{\mathrm{CR}} = {} & |u - u_{\mathrm{CR}}|_{1,h}^2 + 2a(u - \Pi_{\mathrm{P}_1} u, u_{\mathrm{CR}}) - 2\lambda_{\mathrm{CR}}(u - \Pi_{\mathrm{P}_1} u, u_{\mathrm{CR}}) \\ & - \lambda_{\mathrm{CR}} \|u - u_{\mathrm{CR}}\|_{0,\Omega}^2, \end{aligned} \tag{3.14}$$

and the canonical interpolation $\Pi_{\mathrm{P}_1} u$ of the conforming linear element admits the same value of u on each vertex. The main idea here is to rewrite the tricky term $a(u - \Pi_{\mathrm{P}_1} u, u_{\mathrm{CR}})$ by the Green identity as follows:

$$a(u - \Pi_{\mathrm{P}_1} u, u_{\mathrm{CR}}) = \sum_{e \in \mathcal{E}_h^i} \int_e (u - \Pi_{\mathrm{P}_1} u) \left[\frac{\partial u_{\mathrm{CR}}}{\partial n} \right] ds. \tag{3.15}$$

On each interior edge, the interpolation error is approximated by the average of recovered interpolation errors on two adjacent elements.

Define the a posteriori error estimates

$$\begin{aligned} F_{\mathrm{CR},2}^{\mathrm{CR}} = {} & \| K_h \nabla_h u_{\mathrm{CR}} - \nabla_h u_{\mathrm{CR}} \|_{0,\Omega}^2 + 2 \sum_{e \in \mathcal{E}_h^i} \int_e \left\{ P_{\mathrm{P}_1}^K (\nabla_h K_h \nabla_h u_{\mathrm{CR}}) \right\} \left[\frac{\partial u_{\mathrm{CR}}}{\partial n} \right] ds \\ & - 2\lambda_{\mathrm{CR}} \sum_{K \in \mathcal{T}_h} \int_K P_{\mathrm{P}_1}^K (\nabla_h K_h \nabla_h u_{\mathrm{CR}}) u_{\mathrm{CR}} \, dx, \end{aligned} \tag{3.16}$$

$$\begin{aligned} F_{\mathrm{ECR},2}^{\mathrm{ECR}} = {} & \| K_h \nabla_h u_{\mathrm{ECR}} - \nabla_h u_{\mathrm{ECR}} \|_{0,\Omega}^2 + 2 \sum_{e \in \mathcal{E}_h^i} \int_e \left\{ P_{\mathrm{P}_1}^K (\nabla_h K_h \nabla_h u_{\mathrm{ECR}}) \right\} \left[\frac{\partial u_{\mathrm{ECR}}}{\partial n} \right] ds \\ & - 2 \sum_{K \in \mathcal{T}_h} \int_K P_{\mathrm{P}_1}^K (\nabla_h K_h \nabla_h u_{\mathrm{ECR}}) (\Delta_h u_{\mathrm{ECR}} + \lambda_{\mathrm{ECR}} u_{\mathrm{ECR}}) \, dx, \end{aligned} \tag{3.17}$$

with the polynomial $P_{\mathrm{P}_1}^K(\cdot)$ defined in (2.8).

THEOREM 3.3. *Let (λ, u) be an eigenpair of (2.1) with $u \in H^{\frac{7}{2}}(\Omega, \mathbb{R}) \cap H_0^1(\Omega, \mathbb{R})$, and let $(\lambda_{\mathrm{CR}}, u_{\mathrm{CR}})$ and $(\lambda_{\mathrm{ECR}}, u_{\mathrm{ECR}})$ be the corresponding approximate eigenpairs of (2.2) in V_{CR} and V_{ECR}, respectively. The a posteriori error estimates $F_{\mathrm{CR},2}^{\mathrm{CR}}$ in (3.16) and $F_{\mathrm{ECR},2}^{\mathrm{ECR}}$ in (3.17) satisfy*

$$\left| \lambda - \lambda_{\mathrm{CR}} - F_{\mathrm{CR},2}^{\mathrm{CR}} \right| \leq C h^3 |\ln h|^{1/2} |u|_{\frac{7}{2},\Omega}^2, \tag{3.18}$$

$$\left| \lambda - \lambda_{\mathrm{ECR}} - F_{\mathrm{ECR},2}^{\mathrm{ECR}} \right| \leq C h^3 |\ln h|^{1/2} |u|_{\frac{7}{2},\Omega}^2. \tag{3.19}$$

Proof. Thanks to (3.14) and (3.16),

$$\begin{aligned}\lambda - \lambda_{\mathrm{CR}} - F^{\mathrm{CR}}_{\mathrm{CR},2} = |u - u_{\mathrm{CR}}|^2_{1,h} - \| K_h\nabla_h u_{\mathrm{CR}} - \nabla_h u_{\mathrm{CR}} \|^2_{0,\Omega} - \lambda_{\mathrm{CR}}\|u - u_{\mathrm{CR}}\|^2_{0,\Omega}\\ - 2\lambda_{\mathrm{CR}} \sum_{K\in\mathcal{T}_h} \big(u - \Pi_{\mathrm{P}_1} u - P^K_{\mathrm{P}_1}(\nabla^2_h \Pi_{\mathrm{M}} u), u_{\mathrm{CR}}\big)_{0,K}\\ - 2\lambda_{\mathrm{CR}} \sum_{K\in\mathcal{T}_h} \big(P^K_{\mathrm{P}_1}(\nabla^2_h \Pi_{\mathrm{M}} u) - P^K_{\mathrm{P}_1}(\nabla_h K_h \nabla_h u_{\mathrm{CR}}), u_{\mathrm{CR}}\big)_{0,K}\\ + 2a(u - \Pi_{\mathrm{P}_1} u, u_{\mathrm{CR}}) - 2\sum_{e\in\mathcal{E}^i_h} \int_e \big\{P^K_{\mathrm{P}_1}(\nabla_h K_h \nabla_h u_{\mathrm{CR}})\big\}\left[\frac{\partial u_{\mathrm{CR}}}{\partial n}\right] ds.\end{aligned} \tag{3.20}$$

Note that

$$a(u - \Pi_{\mathrm{P}_1} u, u_{\mathrm{CR}}) = \sum_{e\in\mathcal{E}^i_h} \int_e (u - \Pi_{\mathrm{P}_1} u)\left[\frac{\partial u_{\mathrm{CR}}}{\partial n}\right] ds.$$

An analysis similar to the one for Theorem 3.1 leads to

$$\begin{aligned}\lambda - \lambda_{\mathrm{CR}} - F^{\mathrm{CR}}_{\mathrm{CR},2} = 2\sum_{e\in\mathcal{E}^i_h} \int_e \big\{u - \Pi_{\mathrm{P}_1} u - P^K_{\mathrm{P}_1}(\nabla_h K_h \nabla_h u_{\mathrm{CR}})\big\}\left[\frac{\partial (u_{\mathrm{CR}} - u)}{\partial n}\right] ds\\ + Ch^3 |\ln h|^{1/2} |u|^2_{\frac{7}{2},\Omega}.\end{aligned}$$

It follows from (2.5), the Cauchy–Schwarz inequality, and the trace theorem that

$$\begin{aligned}|\lambda - \lambda_{\mathrm{CR}} - F^{\mathrm{CR}}_{\mathrm{CR},2}| \le C \sum_{e\in\mathcal{E}^i_h} \|u - \Pi_{\mathrm{P}_1} u - P^K_{\mathrm{P}_1}(\nabla_h K_h \nabla_h u_{\mathrm{CR}})\|_{0,\omega_e} |u|_{2,\omega_e}\\ + Ch^3 |\ln h|^{1/2} |u|^2_{\frac{7}{2},\Omega}.\end{aligned} \tag{3.21}$$

An analysis similar to the one for Theorem 3.1 proves

$$\sum_{e\in\mathcal{E}^i_h} \|u - \Pi_{\mathrm{P}_1} u - P^K_{\mathrm{P}_1}(\nabla_h K_h \nabla_h u_{\mathrm{CR}})\|_{0,\omega_e} |u|_{2,\omega_e} \le Ch^3 |\ln h|^{1/2} |u|^2_{\frac{7}{2},\Omega}. \tag{3.22}$$

A combination of (3.21) and (3.22) leads to

$$|\lambda - \lambda_{\mathrm{CR}} - F^{\mathrm{CR}}_{\mathrm{CR},2}| \le Ch^3 |\ln h|^{1/2} |u|^2_{\frac{7}{2},\Omega},$$

which completes the proof for (3.18).

For the ECR element,

$$a(u - \Pi_{\mathrm{P}_1} u, u_{\mathrm{ECR}}) = \sum_{e\in\mathcal{E}_h} \int_e (u - \Pi_{\mathrm{P}_1} u)\left[\frac{\partial u_{\mathrm{ECR}}}{\partial n}\right] ds - (u - \Pi_{\mathrm{P}_1} u, \Delta_h u_{\mathrm{ECR}}),$$

with an extra term $(u - \Pi_{\mathrm{P}_1} u, \Delta_h u_{\mathrm{ECR}})$ compared to (3.15) of the CR element. An analysis similar to the one for (3.18) yields

$$\begin{aligned}\lambda - \lambda_{\mathrm{ECR}} - F^{\mathrm{ECR}}_{\mathrm{ECR},2} = -2(u - \Pi_{\mathrm{P}_1} u - P^K_{\mathrm{P}_1}(\nabla_h K_h \nabla_h u_{\mathrm{CR}}), \Delta_h u_{\mathrm{ECR}})\\ + Ch^3 |\ln h|^{1/2} |u|^2_{\frac{7}{2},\Omega}.\end{aligned} \tag{3.23}$$

Since $\|\Delta_h u_{\mathrm{ECR}}\|_{0,\Omega} \le \|\Delta_h(u_{\mathrm{ECR}} - \Pi_{\mathrm{M}} u)\|_{0,\Omega} + \|\Delta_h(\Pi_{\mathrm{M}} u - u)\|_{0,\Omega} + |u|_{2,\Omega}$, it follows from the inverse theorem and (3.6) that

$$\|\Delta_h u_{\mathrm{ECR}}\|_{0,\Omega} \le C(h^{-1}\|\nabla_h(u_{\mathrm{ECR}} - u)\|_{0,\Omega} + h^{-1}\|\nabla_h(u - \Pi_{\mathrm{M}} u)\|_{0,\Omega} + |u|_{2,\Omega} + h|u|_{3,\Omega}).$$

Thanks to (2.6) and (3.6),

$$\|\Delta_h u_{\rm ECR}\|_{0,\Omega} \le C(|u|_{2,\Omega} + h|u|_{3,\Omega}). \tag{3.24}$$

An analysis similar to the one for Theorem 3.1 proves

$$\|u - \Pi_{\rm P_1} u - P_{\rm P_1}^K(\nabla_h K_h \nabla_h u_{\rm CR})\|_{0,\Omega} \le Ch^3 |\ln h|^{1/2} |u|_{\frac{7}{2},\Omega}. \tag{3.25}$$

A combination of (3.23), (3.24), and (3.25) leads to

$$|\lambda - \lambda_{\rm ECR} - F_{\rm ECR,2}^{\rm ECR}| \le Ch^3 |\ln h|^{1/2} |u|_{\frac{7}{2},\Omega}^2,$$

which completes the proof for (3.19). ∎

Compared to the terms in (3.14), the above analysis shows that the terms $\| K_h\nabla_h u_{\rm CR} - \nabla_h u_{\rm CR} \|_{0,\Omega}^2$, $\sum_{e\in\mathcal{E}_h^i}\int_e \{P_{\rm P_1}^K(\nabla_h K_h\nabla_h u_{\rm CR})\}[\frac{\partial u_{\rm CR}}{\partial n}]\,ds$, and $\sum_{K\in\mathcal{T}_h}\int_K P_{\rm P_1}^K(\nabla_h K_h\nabla_h u_{\rm CR}) u_{\rm CR}\,dx$ in the a posteriori error estimate $F_{\rm CR,2}^{\rm CR}$ approximate $|u - u_{\rm CR}|_{1,h}^2$, $a(u - \Pi_{\rm P_1} u, u_{\rm CR})$, and $(u - \Pi_{\rm P_1} u, u_{\rm CR})$ with high accuracy, respectively.

The analysis in Theorem 3.3 for the second type of a posteriori error estimates is of optimal order as verified in Figures 1 and 2. Note that other asymptotically exact a posteriori error estimates can be constructed following (3.16) and (3.17) but with different high accuracy recovered gradients.

4. Postprocessing algorithm. This section proposes two methods to improve accuracy of approximate eigenvalues by employing asymptotically exact a posteriori error estimates.

For ease of presentation, we list the notation of different approximate eigenvalues and a posteriori error estimates. Denote the approximate eigenpairs by the CR element, the ECR element, and the conforming linear element on $\mathcal{T}_h$ by $(\lambda_{\rm CR}, u_{\rm CR})$, $(\lambda_{\rm ECR}, u_{\rm ECR})$, and $(\lambda_{\rm P_1}, u_{\rm P_1})$, respectively. Apply the average-projection method in [14] to the approximate eigenfunctions $u_{\rm CR}$, and denote the resulting eigenfunctions by $\tilde{u}_{\rm P_1^*}$. Define

$$u_{\rm P_1^*} := \tilde{u}_{\rm P_1^*} / \| \tilde{u}_{\rm P_1^*} \|_{0,\Omega} \quad \text{and} \quad \lambda_{\rm P_1^*} := a_h(u_{\rm P_1^*}, u_{\rm P_1^*}). \tag{4.1}$$

Denote the PPR postprocessing technique in [25] by the operator $\overline{K}_h$ and let

$$F_{\rm P_1}^{\rm P_1} := \| \overline{K}_h\nabla u_{\rm P_1} - \nabla u_{\rm P_1} \|_{0,\Omega}^2 .$$

According to [26], $F_{\rm P_1}^{\rm P_1}$ is an asymptotically exact a posteriori error estimate for eigenvalues $\lambda_{\rm P_1}$. Replace the recovered gradient $\overline{K}_h\nabla u_{\rm P_1}$ in the above definition by $K_h\nabla_h u_{\rm CR}$ and $\overline{K}_h\nabla u_{\rm P_1^*}$, and denote the resulting a posteriori error estimates by $F_{\rm P_1}^{\rm CR}$ and $F_{\rm P_1}^{\rm P_1^*}$, respectively. Lemma 2.2 reveals that the error estimate $F_{\rm P_1}^{\rm CR}$ is asymptotically exact.

For eigenvalues by the CR element, replace the recovered gradient $K_h\nabla_h u_{\rm CR}$ in (3.4) by $\overline{K}_h\nabla u_{\rm P_1}$ and $\overline{K}_h\nabla u_{\rm P_1^*}$, and denote the resulting first type of a posteriori error estimates by $F_{\rm CR,1}^{\rm P_1}$ and $F_{\rm CR,1}^{\rm P_1^*}$, respectively. Similarly, replace the recovered gradient $K_h\nabla_h u_{\rm CR}$ in (3.16) by $\overline{K}_h\nabla u_{\rm P_1}$ and $\overline{K}_h\nabla u_{\rm P_1^*}$, and denote the resulting second type of a posteriori error estimates by $F_{\rm CR,2}^{\rm P_1}$ and $F_{\rm CR,2}^{\rm P_1^*}$, respectively. According to [25], the recovered gradient $\overline{K}_h\nabla u_{\rm P_1}$ admits a superconvergence result similar to $K_h\nabla_h u_{\rm CR}$ in (2.10). Thus, both error estimates $F_{\rm CR,1}^{\rm P_1}$ and $F_{\rm CR,2}^{\rm P_1}$ are asymptotically exact too.

TABLE 1
Definitions of recovered eigenvalues and the corresponding convergence rates.

	Recovered gradients	Recovered eigenvalues		Order
λ_{CR}	$K_h\nabla_h u_{\mathrm{CR}}$	$\lambda_{\mathrm{CR},1}^{\mathrm{R,\ CR}} := \lambda_{\mathrm{CR}} + F_{\mathrm{CR},1}^{\mathrm{CR}}$	$\lambda_{\mathrm{CR},2}^{\mathrm{R,\ CR}} := \lambda_{\mathrm{CR}} + F_{\mathrm{CR},2}^{\mathrm{CR}}$	3
	$\overline{K}_h\nabla u_{\mathrm{P}_1}$	$\lambda_{\mathrm{CR},1}^{\mathrm{R,\ P_1}} := \lambda_{\mathrm{CR}} + F_{\mathrm{CR},1}^{\mathrm{P}_1}$	$\lambda_{\mathrm{CR},2}^{\mathrm{R,\ P_1}} := \lambda_{\mathrm{CR}} + F_{\mathrm{CR},2}^{\mathrm{P}_1}$	3
	$\overline{K}_h\nabla u_{\mathrm{P}_1^*}$	$\lambda_{\mathrm{CR},1}^{\mathrm{R,\ P_1^*}} := \lambda_{\mathrm{CR}} + F_{\mathrm{CR},1}^{\mathrm{P}_1^*}$	$\lambda_{\mathrm{CR},2}^{\mathrm{R,\ P_1^*}} := \lambda_{\mathrm{CR}} + F_{\mathrm{CR},2}^{\mathrm{P}_1^*}$	-
λ_{P_1}	$K_h\nabla_h u_{\mathrm{CR}}$	$\lambda_{\mathrm{P}_1}^{\mathrm{R,\ CR}} := \lambda_{\mathrm{P}_1} - F_{\mathrm{P}_1}^{\mathrm{CR}}$		3
	$\overline{K}_h\nabla u_{\mathrm{P}_1}$	$\lambda_{\mathrm{P}_1}^{\mathrm{R,\ P_1}} := \lambda_{\mathrm{P}_1} - F_{\mathrm{P}_1}^{\mathrm{P}_1}$		3
	$\overline{K}_h\nabla u_{\mathrm{P}_1^*}$	$\lambda_{\mathrm{P}_1}^{\mathrm{R,\ P_1^*}} := \lambda_{\mathrm{P}_1} - F_{\mathrm{P}_1}^{\mathrm{P}_1^*}$		-
$\lambda_{\mathrm{P}_1^*}$	$K_h\nabla_h u_{\mathrm{CR}}$	$\lambda_{\mathrm{P}_1^*}^{\mathrm{R,\ CR}} := \lambda_{\mathrm{P}_1^*} - F_{\mathrm{P}_1^*}^{\mathrm{CR}}$		3
	$\overline{K}_h\nabla u_{\mathrm{P}_1}$	$\lambda_{\mathrm{P}_1^*}^{\mathrm{R,\ P_1}} := \lambda_{\mathrm{P}_1^*} - F_{\mathrm{P}_1^*}^{\mathrm{P}_1}$		3
	$\overline{K}_h\nabla u_{\mathrm{P}_1^*}$	$\lambda_{\mathrm{P}_1^*}^{\mathrm{R,\ P_1^*}} := \lambda_{\mathrm{P}_1^*} - F_{\mathrm{P}_1^*}^{\mathrm{P}_1^*}$		-

TABLE 2
Notation for varied combined eigenvalues.

		λ_{P_1}		$\lambda_{\mathrm{P}_1^*}$		
		$F_{\mathrm{P}_1}^{\mathrm{CR}}$	$F_{\mathrm{P}_1}^{\mathrm{P}_1}$	$F_{\mathrm{P}_1^*}^{\mathrm{CR}}$	$F_{\mathrm{P}_1^*}^{\mathrm{P}_1}$	$F_{\mathrm{P}_1^*}^{\mathrm{P}_1^*}$
λ_{CR}	$F_{\mathrm{CR},1}^{\mathrm{CR}}$	$\lambda_{\mathrm{CR,CR},1}^{\mathrm{C,\ P_1}}$	$\lambda_{\mathrm{CR,P_1},1}^{\mathrm{C,\ P_1}}$	$\lambda_{\mathrm{CR,CR},1}^{\mathrm{C,\ P_1^*}}$	$\lambda_{\mathrm{CR,P_1},1}^{\mathrm{C,\ P_1^*}}$	$\lambda_{\mathrm{CR,P_1^*},1}^{\mathrm{C,\ P_1^*}}$
	$F_{\mathrm{CR},2}^{\mathrm{CR}}$	$\lambda_{\mathrm{CR,CR},2}^{\mathrm{C,\ P_1}}$	$\lambda_{\mathrm{CR,P_1},2}^{\mathrm{C,\ P_1}}$	$\lambda_{\mathrm{CR,CR},2}^{\mathrm{C,\ P_1^*}}$	$\lambda_{\mathrm{CR,P_1},2}^{\mathrm{C,\ P_1^*}}$	$\lambda_{\mathrm{CR,P_1^*},2}^{\mathrm{C,\ P_1^*}}$
	$F_{\mathrm{CR},1}^{\mathrm{P}_1}$	$\lambda_{\mathrm{P_1,CR},1}^{\mathrm{C,\ P_1}}$	$\lambda_{\mathrm{P_1,P_1},1}^{\mathrm{C,\ P_1}}$	$\lambda_{\mathrm{P_1,CR},1}^{\mathrm{C,\ P_1^*}}$	$\lambda_{\mathrm{P_1,P_1},1}^{\mathrm{C,\ P_1^*}}$	$\lambda_{\mathrm{P_1,P_1^*},1}^{\mathrm{C,\ P_1^*}}$
	$F_{\mathrm{CR},2}^{\mathrm{P}_1}$	$\lambda_{\mathrm{P_1,CR},2}^{\mathrm{C,\ P_1}}$	$\lambda_{\mathrm{P_1,P_1},2}^{\mathrm{C,\ P_1}}$	$\lambda_{\mathrm{P_1,CR},2}^{\mathrm{C,\ P_1^*}}$	$\lambda_{\mathrm{P_1,P_1},2}^{\mathrm{C,\ P_1^*}}$	$\lambda_{\mathrm{P_1,P_1^*},2}^{\mathrm{C,\ P_1^*}}$

4.1. Recovered eigenvalues. The first approach is to correct the discrete eigenvalues by the corresponding asymptotically exact a posteriori error estimates. A direct application of Theorems 3.1 and 3.3 proves that the accuracy of the resulting recovered eigenvalues is higher than that of the original eigenvalues.

Table 1 lists the definitions of most recovered eigenvalues mentioned in this paper and their theoretical convergence rates. These theoretical convergence rates are direct results from Theorems 3.1 and 3.3, and the superconvergence results of the recovered gradients $K_h\nabla_h u_{\mathrm{CR}}$ and $\overline{K}_h\nabla u_{\mathrm{P}_1}$. Although there is no superconvergence result for the recovered gradient $\overline{K}_h\nabla u_{\mathrm{P}_1^*}$, numerical examples still indicate that the accuracy for the resulting recovered eigenvalues is higher than that of the original eigenvalues.

4.2. Combined eigenvalues. Another way to achieve high accuracy is to take a weighted-average of discrete eigenvalues with the weights computed by the corresponding asymptotically exact a posteriori error estimates. Usually the weighted-average of a lower bound, such as λ_{CR} and λ_{ECR}, and an upper bound, such as λ_{P_1} and $\lambda_{\mathrm{P}_1^*}$c, can achieve better accuracy than those of two lower bounds or two upper bounds.

In this paper, lower bounds for eigenvalues are fixed as λ_{CR}, and upper bounds are λ_{P_1} or $\lambda_{\mathrm{P}_1^*}$ as shown in Table 2. As listed in the first two columns of the table, four different asymptotically exact a posteriori error estimates $F_{\mathrm{CR},1}^{\mathrm{CR}}$, $F_{\mathrm{CR},2}^{\mathrm{CR}}$, $F_{\mathrm{CR},1}^{\mathrm{P}_1}$, and $F_{\mathrm{CR},2}^{\mathrm{P}_1}$ of the lower bound λ_{CR} are considered here to compute the weights. The

first two rows list the two a posteriori error estimates $F_{\mathrm{P}_1}^{\mathrm{CR}}$ and $F_{\mathrm{P}_1}^{\mathrm{P}_1}$ for the upper bound λ_{P_1} and the three a posteriori error estimates $F_{\mathrm{P}_1^*}^{\mathrm{CR}}$, $F_{\mathrm{P}_1^*}^{\mathrm{P}_1}$, and $F_{\mathrm{P}_1^*}^{\mathrm{P}_1^*}$ for the upper bound $\lambda_{\mathrm{P}_1^*}$. The notation for the resulting combined eigenvalues is listed in the lower right block of Table 2. Take the notation $\lambda_{\mathrm{P}_1,\mathrm{CR},1}^{\mathrm{C},\ \mathrm{P}_1^*}$, for example: define

$$\lambda_{\mathrm{P}_1,\mathrm{CR},1}^{\mathrm{C},\ \mathrm{P}_1^*} := \frac{F_{\mathrm{CR},1}^{\mathrm{P}_1}}{F_{\mathrm{CR},1}^{\mathrm{P}_1}+F_{\mathrm{P}_1^*}^{\mathrm{CR}}}\lambda_{\mathrm{P}_1^*}+\frac{F_{\mathrm{P}_1^*}^{\mathrm{CR}}}{F_{\mathrm{CR},1}^{\mathrm{P}_1}+F_{\mathrm{P}_1^*}^{\mathrm{CR}}}\lambda_{\mathrm{CR}}. \tag{4.2}$$

The combined eigenvalues $\lambda_{\mathrm{P}_1,\mathrm{CR},1}^{\mathrm{C},\ \mathrm{P}_1^*}$ are the weighted-average of the upper bound $\lambda_{\mathrm{P}_1^*}$ and the lower bounds λ_{CR}. Note that

$$|\lambda-\lambda_{\mathrm{P}_1^*}+F_{\mathrm{P}_1^*}^{\mathrm{CR}}|\le Ch^3, \tag{4.3}$$

$$|\lambda-\lambda_{\mathrm{CR}}-F_{\mathrm{CR},1}^{\mathrm{P}_1}|\le Ch^3. \tag{4.4}$$

Multiplying (4.3) by $\frac{F_{\mathrm{CR},1}^{\mathrm{P}_1}}{F_{\mathrm{CR},1}^{\mathrm{P}_1}+F_{\mathrm{P}_1^*}^{\mathrm{CR}}}$ and (4.4) by $\frac{F_{\mathrm{P}_1^*}^{\mathrm{CR}}}{F_{\mathrm{CR},1}^{\mathrm{P}_1}+F_{\mathrm{P}_1^*}^{\mathrm{CR}}}$ and adding the results together, we get

$$|\lambda-\lambda_{\mathrm{P}_1,\mathrm{CR},1}^{\mathrm{C},\ \mathrm{P}_1^*}|\le Ch^3.$$

This indicates a third order accuracy of the combined eigenvalues $\lambda_{\mathrm{P}_1,\mathrm{CR},1}^{\mathrm{C},\ \mathrm{P}_1^*}$ in (4.2). The other combined eigenvalues are defined similarly.

The difference between the combined eigenvalues we propose and those in [13] lies in the design of the approximate weights. In [13], two elements, which produce upper bounds and lower bounds of eigenvalues, respectively, are employed to solve eigenvalue problems on two successive meshes. The weights there are computed by the resulting four approximate eigenvalues, while the weights in this paper are computed by the corresponding a posteriori error estimates.

Most of the combined eigenvalues in Table 2 require solving two eigenvalue problems and computing the corresponding a posteriori error estimates, or even one more eigenvalue problem for the recovered gradient. The only exception is the combined eigenvalues $\lambda_{\mathrm{CR},\mathrm{CR},1}^{\mathrm{C},\ \mathrm{P}_1^*}$, $\lambda_{\mathrm{CR},\mathrm{CR},2}^{\mathrm{C},\ \mathrm{P}_1^*}$, $\lambda_{\mathrm{CR},\mathrm{P}_1^*,1}^{\mathrm{C},\ \mathrm{P}_1^*}$, and $\lambda_{\mathrm{CR},\mathrm{P}_1^*,2}^{\mathrm{C},\ \mathrm{P}_1^*}$, since the eigenpair $(\lambda_{\mathrm{P}_1^*},u_{\mathrm{P}_1^*})$ is computed by the projection in [14] of the nonconforming eigenfunction u_{CR}. A third order convergence rate of the resulting combined eigenvalues $\lambda_{\mathrm{CR},\mathrm{CR},1}^{\mathrm{C},\ \mathrm{P}_1^*}$ and $\lambda_{\mathrm{CR},\mathrm{CR},2}^{\mathrm{C},\ \mathrm{P}_1^*}$ is guaranteed by the high accuracy recovered gradient $K_h\nabla_h u_{\mathrm{CR}}$.

5. Numerical examples. This section presents six numerical tests for eigenvalues of the Laplacian operator. The first three examples deal with smooth eigenfunctions, and the other three deal with singular eigenfunctions.

5.1. Adaptive algorithm. There exist some a posteriori error estimates for eigenvalues by nonconforming elements in the literature [10, 20, 21, 30]. The a posteriori error estimates in section 3 can also be employed to improve the accuracy of eigenvalue problems by adaptive algorithms. Starting from an initial grid $\mathcal{T}_1$, the adaptive mesh refinement process operates in the following (widely used) way (see [31]):

1. Set $k=0$.
2. Compute the eigenvalues from (2.2) on $\mathcal{T}_k$ and denote them by $\lambda_{\mathrm{CR}}^{\mathrm{A}}$.

3. Compute the second type of asymptotically exact a posteriori error estimates for eigenvalues. Take the CR element as an example, and compute
(5.1)
$$F_{\mathrm{CR},2}^{\mathrm{CR}} = \| G_h\nabla_h u_{\mathrm{CR}} - \nabla_h u_{\mathrm{CR}} \|_{0,\Omega}^2 + 2\sum_{e\in\mathcal{E}_h^i}\int_e \{P_{\mathrm{P}_1}^K(\nabla_h G_h \nabla_h u_{\mathrm{CR}})\}\left[\frac{\partial u_{\mathrm{CR}}}{\partial n}\right] ds$$
$$-2\lambda_{\mathrm{CR}}\sum_{K\in\mathcal{T}_h}\int_K P_{\mathrm{P}_1}^K(\nabla_h G_h\nabla_h u_{\mathrm{CR}})u_{\mathrm{CR}}\,dx,$$
with the postprocessing operator G_h defined in [11].
4. Compute the local error indicators. In this step, let the local error indicators be the one in [21] as below:
$$\eta_K^2 = \lambda_{\mathrm{CR}}^2 h_K^2 \| u_{\mathrm{CR}} \|_{0,K}^2 + \sum_{e\subset\partial K} h_e \| \left[\frac{\partial u_{\mathrm{CR}}}{\partial n}\right] \|_{0,e}^2 + h_e \| \left[\frac{\partial u_{\mathrm{CR}}}{\partial t}\right] \|_{0,e}^2 \quad (5.2)$$
and $\eta^2 = \sum_{K\in\mathcal{T}} \eta_K^2$.
5. If η is sufficiently small, then stop. Otherwise, refine those elements $K \in \mathcal{T}_k$ with $\eta_K > \theta \max_{K\in\mathcal{T}_k} \eta_K$.
6. Set $k = k + 1$ and go to (2).

Here $0 < \theta < 1$ is a fixed threshold. In the numerical experiments, we always set $\theta = 0.3$. Since the superconvergence result (2.10) for the CR element requires triangulations to be uniform, we use the PPR postprocessing operator G_h in [11] for all adaptive triangulations in this section.

5.2. Example 1. In this example, the model problem (2.1) on the unit square $\Omega = (0,1)^2$ is considered. The exact eigenvalues are

$$\lambda = (m^2 + n^2)\pi^2,\ m,\ n \quad \text{are positive integers,}$$

and the corresponding eigenfunctions are $u = 2\sin(m\pi x_1)\sin(n\pi x_2)$. The domain is partitioned by uniform triangles. The level one triangulation $\mathcal{T}_1$ consists of two right triangles, obtained by cutting the unit square with a northeast line. Each triangulation $\mathcal{T}_i$ is uniformly refined into a half-sized triangulation to get a higher level triangulation $\mathcal{T}_{i+1}$.

Recovered eigenvalues. Figure 1 plots the errors of the first approximate eigenvalues by the CR element, the ECR element, the conforming linear element, and their corresponding recovered eigenvalues.

It shows that the approximate eigenvalues λ_{CR}, λ_{ECR}, and λ_{P_1} converge at a rate of 2; the recovered eigenvalues $\lambda_{\mathrm{CR},\,2}^{\mathrm{R},\,\mathrm{CR}}$ converge at a rate of 3; and the recovered eigenvalues $\lambda_{\mathrm{CR},\,1}^{\mathrm{R},\,\mathrm{CR}}$, $\lambda_{\mathrm{ECR},\,1}^{\mathrm{R},\,\mathrm{ECR}}$, $\lambda_{\mathrm{ECR},\,2}^{\mathrm{R},\,\mathrm{ECR}}$, and $\lambda_{\mathrm{P}_1}^{\mathrm{R},\,\mathrm{P}_1}$ converge at a higher rate of 4. Note that although the theoretical convergence rate of the recovered eigenvalues $\lambda_{\mathrm{CR},\,1}^{\mathrm{R},\,\mathrm{CR}}$, $\lambda_{\mathrm{ECR},\,1}^{\mathrm{R},\,\mathrm{ECR}}$, and $\lambda_{\mathrm{ECR},\,2}^{\mathrm{R},\,\mathrm{ECR}}$ is only 3, numerical tests indicate an even higher convergence rate of 4. The errors of the recovered eigenvalues $\lambda_{\mathrm{CR},\,1}^{\mathrm{R},\,\mathrm{CR}}$, $\lambda_{\mathrm{CR},\,2}^{\mathrm{R},\,\mathrm{CR}}$, $\lambda_{\mathrm{ECR},\,1}^{\mathrm{R},\,\mathrm{ECR}}$, $\lambda_{\mathrm{ECR},\,2}^{\mathrm{R},\,\mathrm{ECR}}$, and $\lambda_{\mathrm{P}_1}^{\mathrm{R},\,\mathrm{P}_1}$ on $\mathcal{T}_8$ are 2.02×10^{-7}, 3.09×10^{-5}, 3.66×10^{-8}, 2.52×10^{-7}, 1.04×10^{-6}, respectively. They are significant improvements on the errors of the approximate eigenvalues λ_{CR}, λ_{ECR}, and λ_{P_1}, which are 3.30×10^{-4}, 9.91×10^{-4}, and 2.97×10^{-3}, respectively. This reveals that the recovered eigenvalues are quite remarkable improvements on the finite element solutions. It shows that the most accurate approximation is $\lambda_{\mathrm{ECR},\,1}^{\mathrm{R},\,\mathrm{ECR}}$, followed by $\lambda_{\mathrm{CR},\,1}^{\mathrm{R},\,\mathrm{CR}}$, $\lambda_{\mathrm{P}_1^*}^{\mathrm{R},\,\mathrm{CR}}$, $\lambda_{\mathrm{P}_1}^{\mathrm{R},\,\mathrm{CR}}$, and $\lambda_{\mathrm{P}_1}^{\mathrm{R},\,\mathrm{P}_1}$. Compared

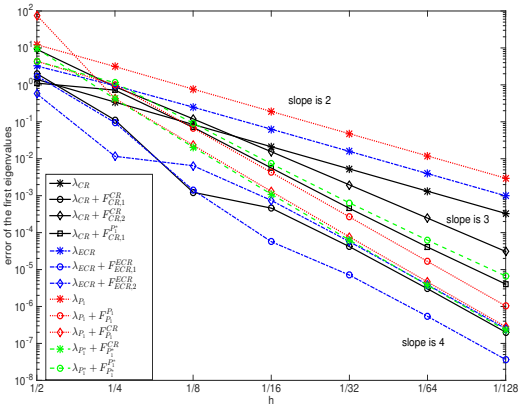

FIG. 1. *The errors of the recovered eigenvalues for Example* 1.

TABLE 3
The errors of different combined eigenvalues on the mesh $\mathcal{T}_8$ *for Example* 1.

	$\lambda^{\mathrm{C,\ P_1}}_{\mathrm{CR,CR},\ 1}$	$\lambda^{\mathrm{C,\ P_1}}_{\mathrm{CR,P_1},\ 1}$	$\lambda^{\mathrm{C,\ P_1^*}}_{\mathrm{CR,CR},\ 1}$	$\lambda^{\mathrm{C,\ P_1^*}}_{\mathrm{CR,P_1},\ 1}$	$\lambda^{\mathrm{C,\ P_1^*}}_{\mathrm{CR,P_1^*},\ 1}$
error	1.53E-07	7.79E-08	1.59E-07	1.35E-08	4.86E-07
	$\lambda^{\mathrm{C,\ P_1}}_{\mathrm{P_1,CR},\ 1}$	$\lambda^{\mathrm{C,\ P_1}}_{\mathrm{P_1,P_1},\ 1}$	$\lambda^{\mathrm{C,\ P_1^*}}_{\mathrm{P_1,CR},\ 1}$	$\lambda^{\mathrm{C,\ P_1^*}}_{\mathrm{P_1,P_1},\ 1}$	$\lambda^{\mathrm{C,\ P_1^*}}_{\mathrm{P_1,P_1^*},\ 1}$
error	1.33E-06	1.25E-06	1.34E-06	1.19E-06	6.90E-07

to the approximation $\lambda^{\mathrm{R,\ CR}}_{\mathrm{P_1},\ }$, the recovered eigenvalue $\lambda^{\mathrm{R,\ CR}}_{\mathrm{P_1^*},\ }$ achieves pretty much the same accuracy but requires solving only one discrete eigenvalue problem.

Combined eigenvalues. The errors of some combined eigenvalues on $\mathcal{T}_8$ are recorded in Table 3. Among all the errors in Table 3, the smallest is 1.35×10^{-8}, and it is the error of a weighted-average of λ_{CR} and $\lambda_{\mathrm{P_1^*}}$, where the weights are computed by $F^{\mathrm{CR}}_{\mathrm{CR},\ 1}$ and $F^{\mathrm{P_1}}_{\mathrm{P_1^*}}$. For the combined eigenvalue $\lambda^{\mathrm{C,\ P_1^*}}_{\mathrm{CR,CR},\ 1}$ on $\mathcal{T}_8$, the error 1.59×10^{-7} is a little larger than the smallest in Table 3, but less computational expense is required.

Extrapolation eigenvalues. Table 4 compares the performance of the recovered eigenvalues and the extrapolation eigenvalues. It shows that the recovered eigenvalue $\lambda^{\mathrm{R,\ CR}}_{\mathrm{CR},\ 1}$ behaves better than the extrapolation eigenvalue $\lambda^{\mathrm{EXP}}_{\mathrm{P_1}}$ but worse than $\lambda^{\mathrm{EXP}}_{\mathrm{CR}}$.

TABLE 4
The errors of the recovered eigenvalues and the extrapolation eigenvalues, where $\lambda^{\mathrm{EXP}}_{\mathrm{CR}} = (4\lambda^h_{\mathrm{CR}} - \lambda^{2h}_{\mathrm{CR}})/3$ *and* $\lambda^{\mathrm{EXP}}_{\mathrm{P_1}} = (4\lambda^h_{\mathrm{P_1}} - \lambda^{2h}_{\mathrm{P_1}})/3$ *are approximate eigenvalues by extrapolation methods.*

h	λ_{CR}	$\lambda_{\mathrm{P_1}}$	$\lambda^{\mathrm{EXP}}_{\mathrm{CR}}$	$\lambda^{\mathrm{EXP}}_{\mathrm{P_1}}$	$\lambda^{\mathrm{R,\ CR}}_{\mathrm{CR},\ 1}$	$\lambda^{\mathrm{R,\ P_1}}_{\mathrm{P_1}}$
$\mathcal{T}_3$	-0.3407	3.1266	1.40E-02	8.18E-02	1.12E-01	1.0103
$\mathcal{T}_4$	-8.47E-02	7.66E-01	6.42E-04	-2.04E-02	1.23E-03	6.77E-02
$\mathcal{T}_5$	-2.11E-02	1.91E-01	3.72E-05	-1.34E-03	-4.61E-04	4.26E-03
$\mathcal{T}_6$	-5.29E-03	4.76E-02	2.28E-06	-8.24E-05	-4.18E-05	2.66E-04
$\mathcal{T}_7$	-1.32E-03	1.19E-02	1.42E-07	-5.12E-06	-3.02E-06	1.66E-05
$\mathcal{T}_8$	-3.30E-04	2.97E-03	8.85E-09	-3.19E-07	-2.02E-07	1.04E-06

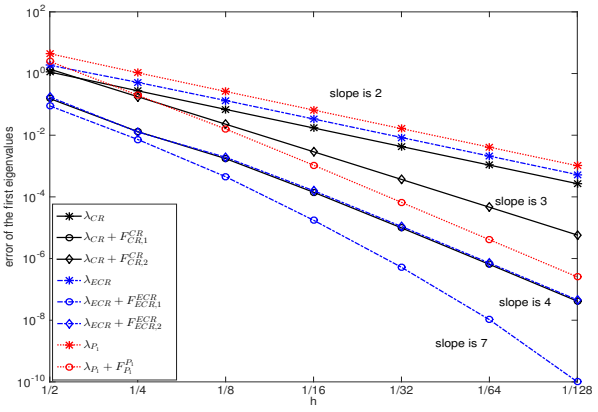

FIG. 2. *The errors of the recovered eigenvalues for Example* 2.

5.3. Example 2: Neumann boundary. Next we consider the eigenvalue problem (2.1) on the unit square $\Omega = (0,1)^2$ with the boundary conditions

$$u|_{x_1=0} = u|_{x_2=0} = u|_{x_2=1} = \partial_{x_1} u|_{x_1=1} = 0.$$

In this case, there exists an eigenpair (λ, u) where $\lambda = \frac{5\pi^2}{4}$, $u = 2\cos\frac{\pi(x_1-1)}{2}\sin\pi x_2$.

We solve this problem on the same sequence of uniform triangulations employed in Example 1. Figure 2 shows that the approximate eigenvalues by the CR element, the ECR element, and the conforming linear element converge at the same rate of 2; the recovered eigenvalue $\lambda^{\mathrm{R,\ CR}}_{\mathrm{CR,\ 2}}$ converges at a rate of 3; and the recovered eigenvalues $\lambda^{\mathrm{R,\ CR}}_{\mathrm{CR,\ 1}}$, $\lambda^{\mathrm{R,\ ECR}}_{\mathrm{ECR,\ 2}}$, and $\lambda^{\mathrm{R,\ P_1}}_{\mathrm{P_1}}$ converge at a rate of 4. In particular, the recovered eigenvalue $\lambda^{\mathrm{R,\ ECR}}_{\mathrm{ECR,\ 1}}$ converges at a strikingly higher rate of 7.

5.4. Example 3: Triangle domain. In this experiment, we consider the eigenvalue problem (2.1) on the domain which is an equilateral triangle:

$$\Omega = \left\{(x_1, x_2) \in \mathbb{R}^2 : 0 < x_2 < \sqrt{3}x_1, \sqrt{3}(1-x_1) < x_2\right\}.$$

The boundary consists of three parts: $\Gamma_1 = \left\{(x_1, x_2) \in \mathbb{R}^2 : x_2 = \sqrt{3}x_1,\ 0.5 \le x_1 \le 1\right\}$, $\Gamma_2 = \left\{(x_1, x_2) \in \mathbb{R}^2 : x_2 = \sqrt{3}(1-x_1),\ 0.5 \le x_1 \le 1\right\}$, and $\Gamma_3 = \left\{(x_1, x_2) \in \mathbb{R}^2 : x_1 = 1,\ 0 \le x_2 \le 1\right\}$. Under the boundary conditions $u|_{\Gamma_1 \cup \Gamma_2} = 0$ and $\partial_{x_1} u|_{\Gamma_3} = 0$, there exists an eigenpair (λ, u), where $\lambda = \frac{16\pi^2}{3}$ and

$$u = \frac{2\sqrt[4]{12}}{3}\left(\sin\frac{4\pi x_2}{\sqrt{3}} + \sin 2\pi\left(x_1 - \frac{x_2}{\sqrt{3}}\right) + \sin 2\pi\left(1 - x_1 - \frac{x_2}{\sqrt{3}}\right)\right).$$

Refine the domain Ω into four half-sized triangles twice and denote the resulting triangulation by $\mathcal{T}_1$. Each triangulation $\mathcal{T}_i$ is uniformly refined into a half-sized triangulation to get a higher level triangulation $\mathcal{T}_{i+1}$. It is shown in Table 5 that the recovered eigenvalues converge much faster than discrete eigenvalues, and the recovered eigenvalue $\lambda^{\mathrm{R,\ CR}}_{\mathrm{CR,\ 1}}$ on $\mathcal{T}_5$ achieves the smallest error 8.80×10^{-9}.

5.5. Example 4: L-shaped domain. Next we consider the eigenvalue problem (2.1) on an L-shaped domain $\Omega = (-1,1)^2/[0,1] \times [-1,0]$. For this problem, the

TABLE 5
The errors and convergence rates of the recovered eigenvalues for Example 3.

	$\mathcal{T}_1$	$\mathcal{T}_2$	$\mathcal{T}_3$	$\mathcal{T}_4$	$\mathcal{T}_5$
$\lambda - \lambda_{\mathrm{CR}}$	3.6697	9.61E-01	2.43E-01	6.10E-02	1.53E-02
$\lambda - \lambda_{\mathrm{CR},\,1}^{\mathrm{R},\,\mathrm{CR}}$	-2.10E-01	-9.46E-03	-2.80E-04	-6.08E-06	-8.80E-09
$\lambda - \lambda_{\mathrm{CR},\,2}^{\mathrm{R},\,\mathrm{CR}}$	6.67E-01	1.11E-01	1.46E-02	1.81E-03	2.24E-04
$\lambda - \lambda_{\mathrm{ECR}}$	4.8974	1.3186	3.36E-01	8.44E-02	2.11E-02
$\lambda - \lambda_{\mathrm{ECR},\,1}^{\mathrm{R},\,\mathrm{ECR}}$	0.3463	2.85E-02	2.27E-03	1.55E-04	1.01E-05
$\lambda - \lambda_{\mathrm{ECR},\,2}^{\mathrm{R},\,\mathrm{ECR}}$	2.12E-03	1.25E-04	3.48E-04	3.28E-05	2.40E-06
$\lambda - \lambda_{\mathrm{P}_1}$	-11.1936	-2.879	-7.29E-01	-1.83E-01	-4.58E-02
$\lambda - \lambda_{\mathrm{P}_1}^{\mathrm{R},\,\mathrm{P}_1}$	1.0209	0.1005	3.49E-03	9.62E-05	2.21E-06

TABLE 6
The relative errors of different approximations to the first eight eigenvalues on $\mathcal{T}_8$ *for Example* 4.

	λ_1	λ_2	λ_3	λ_4	λ_5	λ_6	λ_7	λ_8
λ_{CR}	9.68E-04	9.65E-05	6.69E-05	1.79E-04	8.75E-04	7.75E-04	4.44E-04	3.48E-04
λ_{P_1}	-1.10E-03	-4.52E-04	-6.02E-04	-8.83E-04	-1.37E-03	-1.37E-03	-1.21E-03	-1.23E-03
$\lambda_{\mathrm{P}_1^*}$	-1.41E-03	-4.53E-04	-6.03E-04	-8.85E-04	-1.60E-03	-1.51E-03	-1.21E-03	-1.32E-03
$\lambda_{\mathrm{CR},\,1}^{\mathrm{R},\,\mathrm{CR}}$	4.22E-04	8.29E-07	-1.60E-07	-2.18E-07	3.11E-04	1.80E-04	1.11E-06	-8.53E-07
$\lambda_{\mathrm{CR},\,2}^{\mathrm{R},\,\mathrm{CR}}$	2.41E-05	1.04E-05	8.32E-06	9.85E-06	2.48E-05	1.68E-05	1.70E-05	1.30E-05
$\lambda_{\mathrm{P}_1}^{\mathrm{R},\,\mathrm{P}_1}$	4.78E-04	7.24E-06	8.03E-07	3.35E-06	3.54E-04	2.09E-04	1.72E-05	4.11E-06
$\lambda_{\mathrm{P}_1^*}^{\mathrm{R},\,\mathrm{P}_1^*}$	7.53E-04	7.93E-06	2.46E-06	5.36E-06	5.62E-04	3.28E-04	1.84E-05	8.34E-06
$\lambda_{\mathrm{CR},\mathrm{P}_1,2}^{\mathrm{C},\,\mathrm{P}_1}$	1.94E-04	9.88E-06	7.65E-06	8.80E-06	1.34E-04	7.89E-05	1.70E-05	1.11E-05
$\lambda_{\mathrm{CR},\mathrm{P}_1^*,2}^{\mathrm{C},\,\mathrm{P}_1^*}$	2.46E-04	9.99E-06	7.80E-06	9.13E-06	1.76E-04	1.08E-04	1.73E-05	1.21E-05

third and eighth eigenvalues are known to be $2\pi^2$ and $4\pi^2$, respectively, and the corresponding eigenfunctions are smooth.

In the computation, the level one triangulation is obtained by dividing the domain into three unit squares, each of which is further divided into two triangles. Each triangulation is uniformly refined into a half-sized triangulation to get a higher level triangulation. Since the exact eigenvalues of this problem are unknown, we solve the first eight eigenvalues by the conforming P_3 element on the mesh $\mathcal{T}_9$ and take them as reference eigenvalues.

Table 6 compares the relative errors of the first eight approximate eigenvalues on $\mathcal{T}_8$ by different methods. It implies that the error of the recovered eigenvalue $\lambda_{\mathrm{CR},\,1}^{\mathrm{R},\,\mathrm{CR}}$ is slightly smaller than that of $\lambda_{\mathrm{P}_1}^{\mathrm{R},\,\mathrm{P}_1}$. For the first eigenvalue, the eigenfunction is singular, and the corresponding recovered eigenvalue $\lambda_{\mathrm{CR},\,2}^{\mathrm{R},\,\mathrm{CR}}$ achieves higher accuracy than the recovered eigenvalues $\lambda_{\mathrm{CR},\,1}^{\mathrm{R},\,\mathrm{CR}}$ and $\lambda_{\mathrm{P}_1}^{\mathrm{R},\,\mathrm{P}_1}$. For the third eigenvalue, the corresponding eigenfunction is smooth, and the relative errors of the third recovered eigenvalues $\lambda_{\mathrm{CR},\,1}^{\mathrm{R},\,\mathrm{CR}}$ and $\lambda_{\mathrm{P}_1}^{\mathrm{R},\,\mathrm{P}_1}$ are 1.60×10^{-7} and 8.03×10^{-7}, respectively, smaller than that of the recovered eigenvalue $\lambda_{\mathrm{CR},\,2}^{\mathrm{R},\,\mathrm{CR}}$.

Note that the corresponding eigenfunctions of the third and eighth eigenvalues are smooth, and the other eigenfunctions are singular. Note that the relative errors for recovered eigenvalue $\lambda_{\mathrm{CR},\,2}^{\mathrm{R},\,\mathrm{CR}}$ differ little from each other. However, for $\lambda_{\mathrm{CR},\,1}^{\mathrm{R},\,\mathrm{CR}}$, $\lambda_{\mathrm{P}_1}^{\mathrm{R},\,\mathrm{P}_1}$, and $\lambda_{\mathrm{P}_1^*}^{\mathrm{R},\,\mathrm{P}_1^*}$, the relative errors highly differ for different eigenvalues. This fact implies

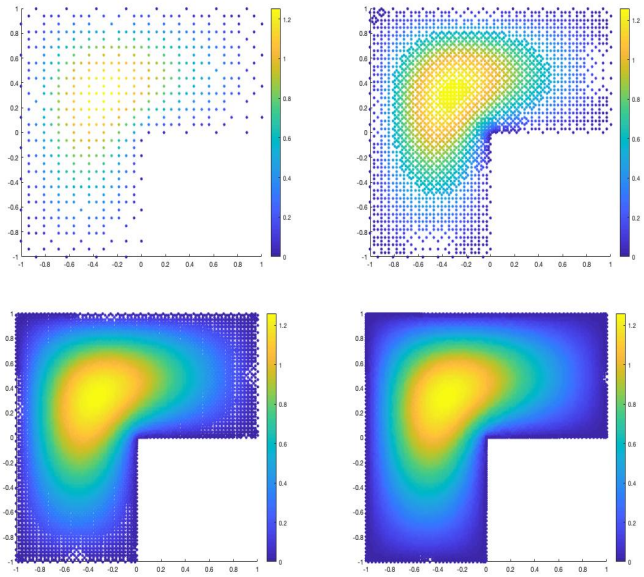

FIG. 3. *The first eigenfunctions on adaptive triangulations with* $k = 5$, $k = 10$, $k = 15$, *and* $k = 20$ *for Example* 4.

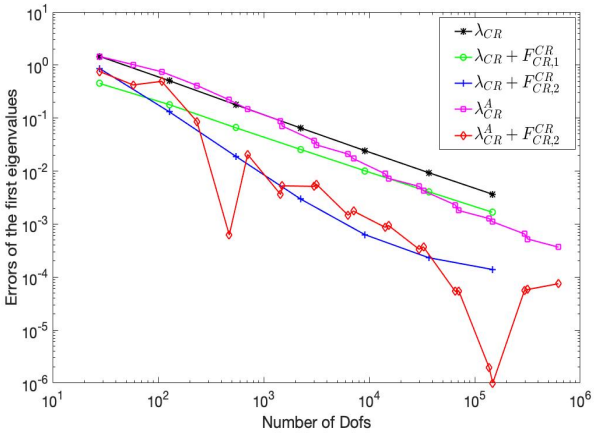

FIG. 4. *The errors of the first eigenvalues for Example* 4.

that the accuracy of the second type error estimates is insensitive to the regularity of the corresponding eigenfunctions, while the accuracy of the first type error estimates relies heavily on the regularity of eigenfunctions.

Figure 3 plots the resulting eigenfunctions on triangulations $\mathcal{T}_5$, $\mathcal{T}_{10}$, $\mathcal{T}_{15}$, and $\mathcal{T}_{20}$ from the adaptive algorithm in section 5.1. Figure 4 plots the relationship between the errors of the first discrete eigenvalues and the sizes of the discrete eigenvalue problems. It shows that the accuracy of the approximate eigenvalues $\lambda^{\mathrm{A}}_{\mathrm{CR}}$ on adaptive triangulations increases faster than that of $\lambda^{\mathrm{R,\ CR}}_{\mathrm{CR,\ 1}}$ on uniform triangulations. The second type a posteriori error estimates on the uniform triangulations are more accurate than those on adaptive triangulations.

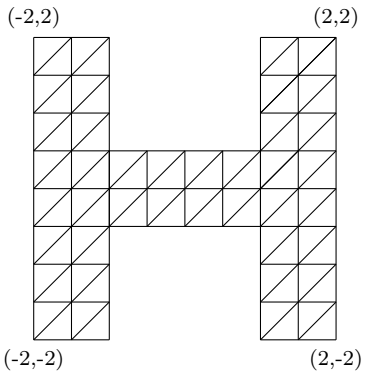

FIG. 5. *Initial triangulation for Example* 5.

TABLE 7
The errors of the first eigenvalue approximations by different methods for Example 5.

h	λ_{CR}	λ_{P_1}	$\lambda_{\mathrm{CR},\,1}^{\mathrm{R},\,\mathrm{CR}}$	$\lambda_{\mathrm{CR},\,2}^{\mathrm{R},\,\mathrm{CR}}$	$\lambda_{\mathrm{P}_1}^{\mathrm{R},\,\mathrm{P}_1}$	$\lambda_{\mathrm{P}_1^*}^{\mathrm{R},\,\mathrm{P}_1^*}$	$\lambda_{\mathrm{CR},\,\mathrm{CR},2}^{\mathrm{C},\,\mathrm{P}_1^*}$
$\mathcal{T}_1$	1.61E+00	-2.84E+00	6.27E-01	4.39E-01	1.93E+00	2.01E+00	6.46E-01
$\mathcal{T}_2$	5.74E-01	-7.99E-01	2.05E-01	6.03E-02	3.37E-01	4.70E-01	1.21E-01
$\mathcal{T}_3$	2.06E-01	-2.54E-01	7.52E-02	8.46E-03	8.76E-02	1.44E-01	3.07E-02
$\mathcal{T}_4$	7.54E-02	-8.68E-02	2.91E-02	9.72E-04	3.04E-02	5.26E-02	1.00E-02
$\mathcal{T}_5$	2.83E-02	-3.10E-02	1.15E-02	8.95E-05	1.17E-02	2.05E-02	3.74E-03
$\mathcal{T}_6$	1.09E-02	-1.15E-02	4.56E-03	2.06E-05	4.61E-03	8.10E-03	1.48E-03

5.6. Example 5: H-shaped domain. Next we consider the eigenvalue problem (2.1) on an H-shaped domain in Figure 5. Note that the first eigenfunction is singular.

The level one triangulation is uniform and shown in Figure 5. Each triangulation is uniformly refined into a half-sized triangulation to get a higher level triangulation. Since the exact eigenvalues of this problem are unknown, the conforming P_3 element is employed to solve the eigenvalue problem on the mesh $\mathcal{T}_9$, and the resulting approximate eigenvalues are taken as reference eigenvalues.

As presented in Table 7, the recovered eigenvalue $\lambda_{\mathrm{CR},\,2}^{\mathrm{R},\,\mathrm{CR}}$ performs better than $\lambda_{\mathrm{CR},\,1}^{\mathrm{R},\,\mathrm{CR}}$ when the eigenfunctions are singular. The errors of $\lambda_{\mathrm{CR},\,1}^{\mathrm{R},\,\mathrm{CR}}$ and $\lambda_{\mathrm{CR},\,2}^{\mathrm{R},\,\mathrm{CR}}$ on $\mathcal{T}_6$ are 4.56×10^{-3} and 2.06×10^{-5}, respectively. The recovered eigenvalue $\lambda_{\mathrm{CR},\,2}^{\mathrm{R},\,\mathrm{CR}}$ on $\mathcal{T}_6$ achieves the smallest error—remarkably smaller than the combined eigenvalue with error 1.48×10^{-3}. The combined eigenvalues behave worse because the asymptotically exact a posteriori error estimates $F_{\mathrm{P}_1^*}^{\mathrm{CR}}$ are less accurate than $F_{\mathrm{CR},\,2}^{\mathrm{CR}}$ when the eigenfunctions are singular.

Figure 6 plots the resulting eigenfunctions on triangulations $\mathcal{T}_2$, $\mathcal{T}_5$, $\mathcal{T}_{10}$, and $\mathcal{T}_{15}$ from the adaptive algorithm in section 5.1. Figure 7 plots the relationship between errors of the first eigenvalues and the sizes of discrete eigenvalue problems. The performance of these approximations is quite similar to that in Example 4. Compared to the first type recovered eigenvalues $\lambda_{\mathrm{CR},\,1}^{\mathrm{R},\,\mathrm{CR}}$ on uniform triangulations, approximate eigenvalue $\lambda_{\mathrm{CR}}^{\mathrm{A}}$ on adaptive triangulations achieves higher accuracy when the size of the discrete problem is large enough. The recovered eigenvalue $\lambda_{\mathrm{CR},\,2}^{\mathrm{R},\,\mathrm{CR}}$ on the uniform triangulations behaves much better than other approximations.

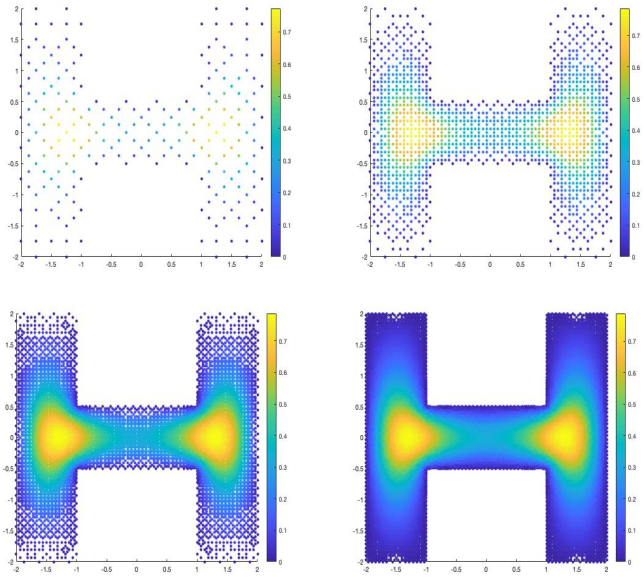

FIG. 6. *The first eigenfunctions on adaptive triangulations with* $k = 2$, $k = 5$, $k = 10$, *and* $k = 15$ *for Example* 5.

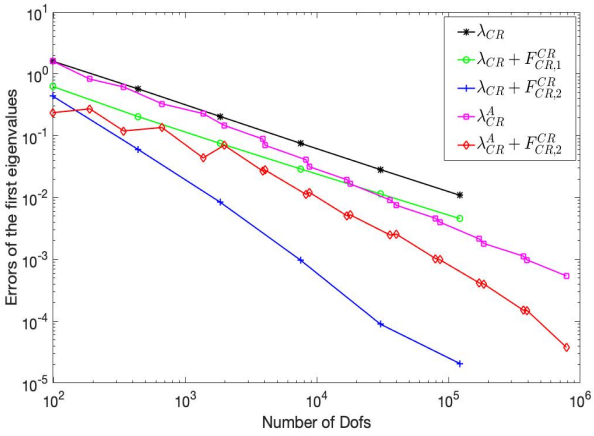

FIG. 7. *The errors of the first eigenvalue for Example* 5.

5.7. Example 6: Hollow-shaped domain. Consider the eigenvalue problem (2.1) with the boundary condition

$$u|_{\Gamma_D} = 0 \text{ and } \partial_{x_1} u|_{\Gamma_N} = 0$$

on a hollow-shaped domain in Figure 8 with $\Gamma_N = \{(x_1, x_2) : x_1 = -1, -1 \le x_2 \le 1\}$ and $\partial\Omega = \Gamma_D \cup \Gamma_N$. Note that the first eigenfunction is singular.

The level one triangulation is uniform and shown in Figure 8. Each triangulation is uniformly refined into a half-sized triangulation to get a higher level triangulation. Since the exact eigenvalues of this problem are unknown, the conforming P_3 element is employed to solve the eigenvalue problem on the mesh $\mathcal{T}_9$, and the resulting approximate eigenvalues are taken as reference eigenvalues.

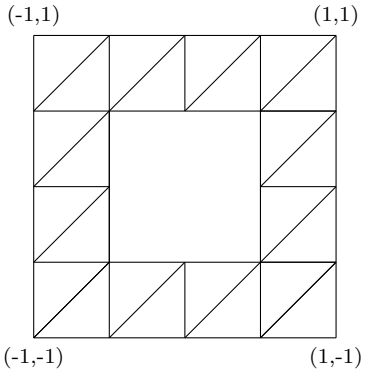

FIG. 8. *Initial triangulation for Example* 6.

TABLE 8
The errors of the first eigenvalue approximations by different methods for Example 6.

h	λ_{CR}	λ_{P_1}	$\lambda_{\mathrm{CR},\ 1}^{\mathrm{R},\ \mathrm{CR}}$	$\lambda_{\mathrm{CR},\ 2}^{\mathrm{R},\ \mathrm{CR}}$	$\lambda_{\mathrm{P}_1}^{\mathrm{R},\ \mathrm{P}_1}$	$\lambda_{\mathrm{P}_1^*}^{\mathrm{R},\ \mathrm{P}_1^*}$	$\lambda_{\mathrm{CR},\ \mathrm{P}_1,2}^{\mathrm{C},\ \mathrm{P}_1}$
$\mathcal{T}_2$	6.42E-01	-1.32E+00	1.28E-01	1.14E-01	7.16E-01	8.76E-01	2.38E-01
$\mathcal{T}_3$	2.23E-01	-3.84E-01	6.93E-02	2.08E-02	1.24E-01	1.80E-01	5.02E-02
$\mathcal{T}_4$	7.99E-02	-1.19E-01	2.81E-02	2.74E-03	3.44E-02	5.64E-02	1.33E-02
$\mathcal{T}_5$	2.94E-02	-3.90E-02	1.12E-02	3.77E-04	1.21E-02	2.08E-02	4.63E-03
$\mathcal{T}_6$	1.11E-02	-1.34E-02	4.53E-03	1.14E-04	4.68E-03	8.12E-03	1.85E-03
$\mathcal{T}_7$	4.32E-03	-4.72E-03	1.87E-03	9.75E-05	1.90E-03	3.26E-03	7.99E-04

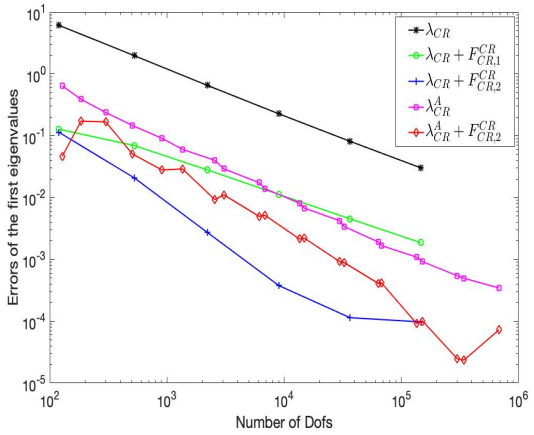

FIG. 9. *The errors of the first eigenvalues for Example* 6.

Table 8 lists the errors of the approximate eigenvalues on each mesh by different methods. The recovered eigenvalue $\lambda_{\mathrm{CR},\ 2}^{\mathrm{R},\ \mathrm{CR}}$ performs remarkably better than all of the other recovered eigenvalues and combined eigenvalues when the eigenfunctions are singular. The error of the recovered eigenvalue $\lambda_{\mathrm{CR},\ \mathrm{P}_1,2}^{\mathrm{C},\ \mathrm{P}_1}$ on $\mathcal{T}_7$ is 7.99×10^{-4}, and it is smaller than all of the other approximations except for $\lambda_{\mathrm{CR},\ 2}^{\mathrm{R},\ \mathrm{CR}}$. It implies that if the corresponding eigenfunctions are not smooth enough, the second type of asymptotically exact a posteriori error estimate $F_{\mathrm{CR},\ 2}^{\mathrm{CR}}$ admits higher accuracy than $F_{\mathrm{CR},\ 1}^{\mathrm{CR}}$.

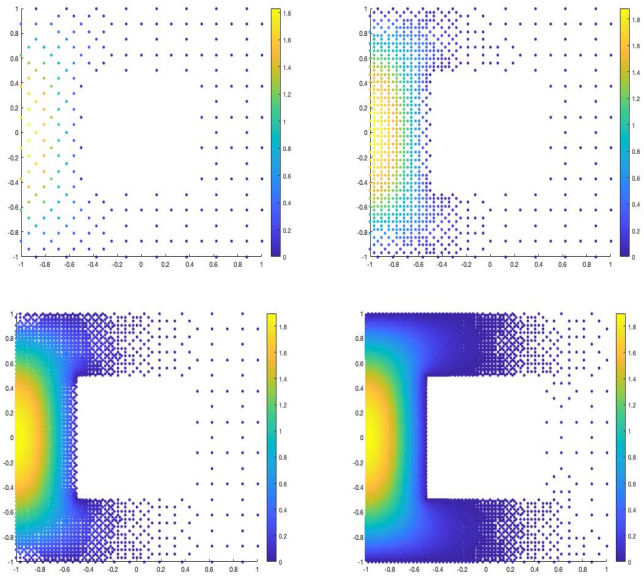

FIG. 10. *The first eigenfunctions on adaptive triangulations with* $k = 2$, $k = 5$, $k = 10$, *and* $k = 15$ *for Example* 6.

Figure 9 plots the relationship between errors of the first eigenvalues and the sizes of discrete eigenvalue problems. Figure 10 plots the resulting eigenfunctions on triangulations $\mathcal{T}_2$, $\mathcal{T}_5$, $\mathcal{T}_{10}$, and $\mathcal{T}_{15}$ from the adaptive algorithm in section 5.1. The performance of these approximations is quite similar to that in Examples 4 and 5. The second type of recovered eigenvalues on uniform triangulations achieves remarkably higher accuracy than most of the other approximations.

REFERENCES

[1] M. AINSWORTH AND J. T. ODEN, *A Posteriori Error Estimation in Finite Element Analysis*, Pure Appl. Math., John Wiley & Sons, New York, 2000.

[2] I. BABUŠKA AND W. C. RHEINBOLDT, *A-posteriori error estimates for the finite element method*, Internat. J. Numer. Methods Engrg., 12 (1978), pp. 1597–1615, https://doi.org/10.1002/nme.1620121010.

[3] I. BABUŠKA, T. STROUBOULIS, C. UPADHYAY, S. GANGARAJ, AND K. COPPS, *Validation of a posteriori error estimators by numerical approach*, Internat. J. Numer. Methods Engrg., 37 (1994), pp. 1073–1123, https://doi.org/10.1002/nme.1620370702.

[4] R. BECKER, S. MAO, AND Z. SHI, *A convergent nonconforming adaptive finite element method with quasi-optimal complexity*, SIAM J. Numer. Anal., 47 (2010), pp. 4639–4659, https://doi.org/10.1137/070701479.

[5] J. H. BRANDTS, *Superconvergence and a posteriori error estimation for triangular mixed finite elements*, Numer. Math., 68 (1994), pp. 311–324, https://doi.org/10.1007/s002110050064.

[6] C. CARSTENSEN, *All first-order averaging techniques for a posteriori finite element error control on unstructured grids are efficient and reliable*, Math. Comp., 73 (2004), pp. 1153–1165, https://doi.org/10.1090/S0025-5718-03-01580-1.

[7] C. CARSTENSEN AND J. HU, *A unifying theory of a posteriori error control for nonconforming finite element methods*, Numer. Math., 107 (2007), pp. 473–502, https://doi.org/10.1007/s00211-007-0068-z.

[8] C. CARSTENSEN, J. HU, AND A. ORLANDO, *Framework for the a posteriori error analysis of nonconforming finite elements*, SIAM J. Numer. Anal., 45 (2007), pp. 68–82, https://doi.org/10.1137/050628854.

[9] M. CROUZEIX AND P.-A. RAVIART, *Conforming and nonconforming finite element meth-*

ods for solving the stationary Stokes equations I, Rev. Française Automat. Informat. Recherche Opérationnelle Sér. Rouge, 7 (1973), pp. 33–75, https://doi.org/10.1051/m2an/197307r300331.

[10] R. G. Durán, C. Padra, and R. Rodríguez, *A posteriori error estimates for the finite element approximation of eigenvalue problems*, Math. Models Methods Appl. Sci., 13 (2003), pp. 1219–1229, https://doi.org/10.1142/S0218202503002878.

[11] H. Guo and Z. Zhang, *Gradient recovery for the Crouzeix–Raviart element*, J. Sci. Comput., 64 (2015), pp. 456–476, https://doi.org/10.1007/s10915-014-9939-5.

[12] J. Hu, Y. Huang, and Q. Lin, *Lower bounds for eigenvalues of elliptic operators: By nonconforming finite element methods*, J. Sci. Comput., 61 (2014), pp. 196–221, https://doi.org/10.1007/s10915-014-9821-5.

[13] J. Hu, Y. Huang, and Q. Shen, *A high accuracy post-processing algorithm for the eigenvalues of elliptic operators*, J. Sci. Comput., 52 (2012), pp. 426–445, https://doi.org/10.1007/s10915-011-9552-9.

[14] J. Hu, Y. Huang, and Q. Shen, *Constructing both lower and upper bounds for the eigenvalues of elliptic operators by nonconforming finite element methods*, Numer. Math., 131 (2015), pp. 273–302, https://doi.org/10.1007/s00211-014-0688-z.

[15] J. Hu and L. Ma, *Asymptotic Expansions of Eigenvalues by both the Crouzeix–Raviart and Enriched Crouzeix–Raviart Elements*, preprint, https://arxiv.org/abs/1902.09524, 2019.

[16] J. Hu, L. Ma, and R. Ma, *Optimal Superconvergence Analysis for the Crouzeix-Raviart and the Morley Elements*, preprint, https://arxiv.org/abs/1808.09810, 2018.

[17] J. Hu and R. Ma, *Superconvergence of both the Crouzeix–Raviart and Morley elements*, Numer. Math., 132 (2016), pp. 491–509, https://doi.org/10.1007/s00211-015-0729-2.

[18] Y. Huang and J. Xu, *Superconvergence of quadratic finite elements on mildly structured grids*, Math. Comp., 77 (2008), pp. 1253–1268, https://doi.org/10.1090/S0025-5718-08-02051-6.

[19] Y. Huang and N. Yi, *The superconvergent cluster recovery method*, J. Sci. Comput., 44 (2010), pp. 301–322, https://doi.org/10.1007/s10915-010-9379-9.

[20] M. G. Larson, *A posteriori and a priori error analysis for finite element approximations of self-adjoint elliptic eigenvalue problems*, SIAM J. Numer. Anal., 38 (2000), pp. 608–625, https://doi.org/10.1137/S0036142997320164.

[21] Y. Li, *A posteriori error analysis of nonconforming methods for the eigenvalue problem*, J. Syst. Sci. Complex., 22 (2009), pp. 495–502, https://doi.org/10.1007/s11424-009-9181-7.

[22] Y.-W. Li, *Global superconvergence of the lowest-order mixed finite element on mildly structured meshes*, SIAM J. Numer. Anal., 56 (2018), pp. 792–815, https://doi.org/10.1137/17M112587X.

[23] Q. Lin and A. Zhou, *Notes on superconvergence and its related topics*, J. Comput. Math., 11 (1993), pp. 211–214.

[24] L. S. D. Morley, *The triangular equilibrium element in the solution of plate bending problems*, Aeronaut. Quart., 19 (1968), pp. 149–169, https://doi.org/10.1017/S0001925900004546.

[25] A. Naga and Z. Zhang, *A posteriori error estimates based on the polynomial preserving recovery*, SIAM J. Numer. Anal., 42 (2004), pp. 1780–1800, https://doi.org/10.1137/S0036142903413002.

[26] A. Naga, Z. Zhang, and A. Zhou, *Enhancing eigenvalue approximation by gradient recovery*, SIAM J. Sci. Comput., 28 (2006), pp. 1289–1300, https://doi.org/10.1137/050640588.

[27] R. Rannacher, *Nonconforming finite element methods for eigenvalue problems in linear plate theory*, Numer. Math., 33 (1979), pp. 23–42, https://doi.org/10.1007/BF01396493.

[28] P.-A. Raviart and J.-M. Thomas, *A mixed finite element method for second order elliptic problems*, in Mathematical Aspects of Finite Element Methods (Proc. Conf., Consiglio Naz. delle Ricerche (C.N.R.), Rome, 1975), Lecture Notes in Math. 606, Springer, Berlin, 1977, pp. 292–315.

[29] Z.-C. Shi and M. Wang, *The Finite Element Method*, Science Press, Beijing, 2010 (in Chinese).

[30] R. Verfürth, *A posteriori error estimates for nonlinear problems: Finite element discretizations of elliptic equations*, Math. Comp., 62 (1994), pp. 445–475, https://doi.org/10.1090/S0025-5718-1994-1213837-1.

[31] R. Verfürth, *A Review of A Posteriori Error Estimation and Adaptive Mesh-Refinement Techniques*, Wiley-Teubner, London, UK, 1996.

[32] N. Yan and A. Zhou, *Gradient recovery type a posteriori error estimates for finite element approximations on irregular meshes*, Comput. Methods Appl. Mech. Engrg., 190 (2001), pp. 4289–4299, https://doi.org/10.1016/s0045-7825(00)00319-4.

[33] Y.-D. Yang, *A posteriori error estimates in Adini finite element for eigenvalue problems*, J. Comput. Math., 18 (2000), pp. 413–418.

[34] Z. Zhang and A. Naga, *A new finite element gradient recovery method: Superconvergence*

property, SIAM J. Sci. Comput., 26 (2005), pp. 1192–1213, https://doi.org/10.1137/S1064827503402837.

[35] O. C. Zienkiewicz and J. Zhu, *The superconvergent patch recovery and a posteriori error estimates: Part* 1: *The recovery technique*, Internat. J. Numer. Methods Engrg., 33 (1992), pp. 1331–1364, https://doi.org/10.1002/nme.1620330702.

[36] O. C. Zienkiewicz and J. Zhu, *The superconvergent patch recovery and a posteriori error estimates: Part* 2: *Error estimates and adaptivity*, Internat. J. Numer. Methods Engrg., 33 (1992), pp. 1365–1382, https://doi.org/10.1002/nme.1620330703.